03942-7-T

CM-979

THE UNIVERSITY OF MICHIGAN

COLLEGE OF ENGINEERING
Department of Aeronautical and Astronautical Engineering

Technical Report

JET INTERFERENCE EXPERIMENTS EMPLOYING BODY-ALONE AND BODY-FIN CONFIGURATIONS AT SUPERSONIC SPEEDS

Gerard F. Carvalho
Paul B. Hays

UMRI Project 03942

under contract with:

DEPARTMENT OF THE NAVY
BUREAU OF NAVAL WEAPONS
CONTRACT NO. NOrd-16595
WASHINGTON, D. C.

through:

APPLIED PHYSICS LABORATORY
THE JOHNS HOPKINS UNIVERSITY
SILVER SPRING, MARYLAND

administered by:

THE UNIVERSITY OF MICHIGAN RESEARCH INSTITUTE ANN ARBOR

December 1960

ABSTRACT

An experimental investigation of the side-jet, supersonic stream interaction phenomena has shown that beneficial interaction forces can be obtained on a body of revolution with or without fins. The magnitude of the interaction forces obtained on a body of revolution with fins can exceed the jet static thrust, while the magnitude of the interaction forces obtained on a body of revolution without fins is much less. This investigation has also shown that some of the important parameters governing the magnitude of the interaction force obtained on a body of revolution are fin-exposed semi-span, side-jet nozzle geometry, and side-jet nozzle location.

TABLE OF CONTENTS

LIST OF FIGURES

LIST OF FIGURES (Concluded)

LIST OF SYMBOLS

A_b base area.

A_t nozzle-throat area.

b exposed semi-span of fin.

c root chord of fin.

C_{N_Δ} total normal force coefficient $= \frac{N_\Delta}{qA_b}$.

C_t nozzle-thrust coefficient $= \frac{N_V}{p_{o_j} A_t}$.

d nozzle-throat diameter.

D base diameter.

I impulse $= \frac{N_\Delta}{\dot{m}}$.

K magnification factor $= \frac{N_\Delta}{N_V}$.

ℓ_s distance of separation line ahead of body base.

L body length.

$\dot{m}$ measured mass flow.

$\dot{m}_{inv}$ inviscid mass flow.

M_∞ free-stream Mach number.

M_j nozzle-exit Mach number.

$\dot{M}$ mass-flow parameter $= \frac{\dot{m}}{\rho V A_b}$.

N_I interaction force $= (K - 1)N_V$.

N_V jet thrust in a vacuum.

N_Δ normal force increment due to jet (normal force on body in supersonic flow with jet on, minus normal force in supersonic flow with jet off).

p free-stream static pressure.

p_a static pressure for calibration tests.

p_o free-stream total pressure.

p_{o_j} jet stagnation pressure.

q free-stream dynamic pressure = $\frac{\gamma}{2}pM^2$.

R_e free-stream Reynolds number based on body length L.

R_{e_d} jet Reynolds number based on conditions at nozzle throat.

T free-stream static temperature.

V free-stream velocity.

X distance from body nose to nozzle centerline.

X' distance from nozzle centerline to body base.

$\bar{X}$ distance upstream from nozzle centerline to center of pressure of total normal force N_Δ.

γ ratio of specific heats.

Φ angle between vertical plane of symmetry and fin.

ρ free-stream density.

INTRODUCTION

In recent years, flight to and beyond the outer reaches of the earth's atmosphere has been given increasingly serious consideration. One realizes immediately the need for vehicle control if a vehicle is to follow any path other than a ballistic path. Vehicle control within the earth's atmosphere is generally provided by aerodynamic controls, while outside the earth's atmosphere jet reaction controls are needed. But little is known about vehicle control in the intermediate region where aerodynamic controls lose their effectiveness and jet reaction controls produce some type of aerodynamic interference. It is the purpose of this report to present the results of a program designed to investigate the feasibility of side jets as control devices within the atmosphere.

An experimental investigation into the use of side jets as control devices was begun at the Aeronautical Engineering Laboratories of The University of Michigan in 1950.[1,2] Early test results indicated that an interaction force, complementary to the jet force, can be obtained when a jet nozzle is exhausted from a body into a supersonic stream. These results also revealed that the magnitude of the interaction force depends, among other things, on nozzle geometry and nozzle location relative to the base of the body.

Recent tests of side jets issuing from flat plates[3] have revealed beneficial interaction forces several times as large as those observed on bodies of revolution. These large interaction forces on flat plates are due to the fact that the region of high pressures ahead of the jet cannot propagate to the

opposite side of the body and oppose the jet force, as happens on a body of revolution. If fins are added to a body of revolution, however, so as to prevent the circumferential spreading of the high-pressure region ahead of the jet, then interaction forces comparable to those found on a flat plate can be expected.

The present tests were conducted to determine the effects of fins and of changes in nozzle geometry and location on the interaction force produced by a side jet issuing from a body of revolution into a supersonic stream.

EXPERIMENTAL EQUIPMENT

Wind Tunnel.—The experimental data were obtained in The University of Michigan's 8- by 13-in. supersonic wind tunnel. This wind tunnel is of the blow-down type, with throttling valves located between the dry-air storage tank and the stagnation chamber to allow tunnel operation at atmospheric or sub-atmospheric stagnation pressures. The test Mach numbers were $M_\infty = 2.43$ and $M_\infty = 3.97$. The Reynolds number was varied at both Mach numbers by means of the above-mentioned throttling valves. The Reynolds number variation was 0.258×10^6 per inch to 0.399×10^5 per inch at $M_\infty = 2.43$ and the variation was 0.127×10^6 per inch to 0.707×10^5 per inch at $M_\infty = 3.97$. Wind tunnel calibration data and a description of the facility are contained in Refs. 4 and 5.

Models.—The models tested were ogive cylinders of two different lengths. The long model, shown in Figure 1, had a fineness ratio of 6.5 and was used for all the tests with fins. Sonic nozzles and a 90° supersonic slot were tested with this model. The sonic nozzles had rounded entrances, and exit diameters of 0.172 in. These exit ports were tested in groups of one, two, or three, symmetrically arranged between a pair of fins. The 90° supersonic slot had a cross section consisting of a rounded entrance, a (parallel) throat of 0.020-in. width, and a straight-sided downstream section with an included divergence angle of 23°. This nozzle produced a theoretical exit Mach number of 3.74.

The long model was also used for tests of a nose jet. This jet issued from a sonic nozzle, with sharp entrance, located 1.225 in. from the nose and inclined 13° forward from the vertical. When not in use, this nozzle was

plugged and the model surface was smoothed with modeling clay.

The short model (Figure 2) had a fineness ratio of 4.5. Like the long model, it had a fineness-ratio-3 ogive nose and a cylindrical afterbody of approximately 2-inch diameter. This model was used for tests of various single aft nozzles. The nozzles used with this model consisted of three rounded-entrance sonic nozzles 0.119, 0.160, and 0.224 in. in diameter, a sharp-entrance nozzle 0.160-in. in diameter, and two conical nozzles. The larger conical nozzle had a slightly rounded entrance and a theoretical exit Mach number of approximately $M_j = 2.95$. The smaller conical nozzle had a more gradual entrance and gave a theoretical exit Mach number of $M_j = 3.07$. The afterbody behind the nozzle centerline varied from 0.50 to 1.75 in.

Internal adapters allowed both models to be mounted on the sting balance (shown in Figure 3) so that the model served as a windshield to the strain-gauge bridges. In this manner a ratio of sting diameter to model base diameter equal to 0.30 was obtained. The sting was tapered and at its root had a ratio of sting diameter to model base diameter of 0.437. The ratio of sting length to model base diameter was 3.00.

Tests.—The forces on the models produced by the jet and the jet-supersonic-main-stream interaction were measured by the sting balance. The increment of force on the model due to the jet force and the interaction force was obtained by turning the jet on after the supersonic flow had started in the tunnel and then turning the jet off before the tunnel was shut down. The time allowed between starting and stopping the tunnel flow and jet flow was always of sufficient duration (a few seconds) to obtain steady-state force measurements.

The strains in the cantilever beam produced by the forces on the model were sensed by two Wheatstone bridge circuits. An electronic system comprised of commercial carrier amplifiers and an oscillograph amplified and recorded the output signals of the two bridges. Frequent calibration checks were obtained by hanging known weights on the models, thus producing known moments on the sting balance. The outputs from the bridges due to the weights were recorded by the oscillograph. In this manner a constant check of the balance system sensitivity and stability was obtained.

All tests were conducted with the model at zero angle of attack. The results of earlier testing at various angles of attack[2] showed only slight variation in the total force normal to the model surface within an angle of attack range of -12° to +14°.

The boundary layer over the model remained laminar throughout the range of Reynolds numbers and Mach numbers of the tests. A turbulent boundary layer was obtained for some of the tests by installing an "O" ring on the nose of the model. This "O" ring was 0.065 in. thick and was located approximately 0.5 in. behind the nose of the model.

The jet-stagnation-pressure probe and temperature-sensing thermocouple were located inside the model stagnation chamber. The model stagnation chamber was considered to be the space between the model outer shell and the internal adapter. The jet stagnation pressure was measured by a laboratory-test pressure gauge. The gauge could measure pressures and partial vacuums with an accuracy of 0.25%. The jet stagnation temperature was measured with an accuracy of approximately ±1% by a thermocouple potentiometer. The jet gas for these

tests was air obtained from a laboratory air supply.

The mass flow through the various nozzles was measured with a commercial ASME sharp-edge orifice. The meter run was a steel tube of 1-1/2-in. standard pipe size with lengths of 40 pipe diameters upstream and 11 pipe diameters downstream of the orifice plate. The orifice-to-pipe-diameter ratio was 0.200. The coefficients used in the reduction of the mass-flow data were obtained from Ref. 6.

Discussion of Errors.—An analysis of the repeatability of the calibration data for the sting balance system showed a scatter band of approximately ±1% width. A similar analysis indicated the scattering band width of the force measurements was approximately ±3% under actual test conditions. The mass-flow measuring equipment, designed according to ASME standards, was accurate within ±1%. It should be noted that these deviations are representative of the mid-range measurements. Measurements of smaller forces and mass flows are subject to slightly greater error and measurements in the high range are considerably more accurate.

DISCUSSION OF TEST RESULTS

Qualitative Description of Interaction Phenomenon.—When a jet is exhausted from the surface of a body immersed in a supersonic stream, the jet acts as an obstruction to the flow. The shock wave ahead of the jet is somewhat similar to the shock wave ahead of a blunt body. Between the shock wave and the jet, there exists a high-pressure zone. Since this shock-wave and high-pressure zone is in close proximity to the body and interacts with the boundary layer, the boundary layer on the body generally separates. Thus the interaction between the side jet and the supersonic stream creates a separation zone on the body surface. The high pressures contained within the separated region exert a force on the body in addition to the force of the jet.

In a flat-plate investigation of this phenomenon,[3] the separation was found to spread much more rapidly in the lateral direction than in the free-stream direction. On the flat plate, where the span of the plate was greater than the distance which the separation spread laterally, it was possible to obtain interaction forces equal to and greater than the jet forces. Experiments have shown that it is not possible to obtain interaction forces on a body of revolution without fins as large as those obtainable on a flat plate. This loss in the interaction force appears to be related to the lateral spreading of the separated zone around the body. As the separated zone spreads laterally, it also travels circumferentially around the body (see Figures 4a and 4b). When the separated zone completely surrounds the body, a major portion of the beneficial interaction is cancelled.

Consider now the result of restricting (by fins) the lateral spreading of the separated zone on a body of revolution. The high-pressure region between the shock wave that surrounds the jet of gas issuing from the body and the jet surface acts as a "source" which forces air into the boundary layer and causes it to separate. The "source" air has two means of escaping from the restricted separation zone. First, it may escape through mixing at the top of the separation zone, and second, through the base area of the separation zone. With the addition of fins to the body of revolution the separation zone, and hence the possible mixing area, is reduced. When, moreover, the fins are added to the body, thus restricting the lateral spread of separation, the base area on each side of the jet through which air in the separation zone could escape downstream is reduced. Hence only two possibilities exist for the accommodation of the air forced into the separation zone. First, the pressure within the separated zone may increase, thus reducing the amount of air forced into this zone. Secondly, the separated zone may expand in the stream direction, thus increasing the mixing zone. Both effects seem to occur at the same time. The separation zone on the top of the body between the fins expands in the streamwise direction and the pressures within the separation zone increase. In addition, the detrimental separation on the underside of the body is prevented by the fins. Thus the interaction force obtained on a body of revolution with fins is greater than the interaction force obtained on a body of revolution without fins.

In the realistic case, the above-mentioned mechanism is not fully realized because of the influence of the boundary layer on the fins. The separation zone may cover the fins as well as the body, thus presenting the possibility of air

flow over the leading edge of the fins and the creation of a high-pressure zone on the underside of the fins, if the fin leading edge is subsonic. Also, when the obstruction created by the jet becomes sufficiently large, the separation zone will reach the forward apices of the fins and cause the air to separate on the underside of the fins and on the side of the body, with resultant diminution in the interaction force.

In review, then, the following qualitative picture of the interaction force can be developed. At extremely low jet pressures the interaction force will be very similar for all bodies, with or without fins, because the separation zone will be small and will be contained on the jet side of the body. As the momentum of the jet increases, the separation zone will grow and spread circumferentially around the body, resulting in a loss of interaction force on a body of revolution without fins. The separation zone (and interaction force) on a body of revolution with fins will continue to grow until either the separation reaches the apices of the fins or flows over the leading edge of the fins. Then, for the fin-body configuration, the growth of the ratio of the interaction force to the pure-jet reaction will decrease with further increases in the jet momentum.

Configurations with Fins.—A comparison of the interaction forces obtained on a body of revolution with and without fins is shown in Figure 5. The curve for the body alone shows a slight increase in C_{N_Δ} due to the interaction; but the addition of fins causes a much greater increase in C_{N_Δ}. It is interesting to note that the interaction is only slightly dependent upon the fin chord and rather sensitive to fin span. This trend is apparent from the comparison of the forces obtained with the 1-in.-span fins of various chords with the 2-in.-span

fins; these test data seem to support the earlier statement that the separation of the boundary layer, due to the jet, spreads much more rapidly in the lateral direction than it does in the streamwise direction. One is led to the conclusion that a loss in interaction is caused by flow seeping around the leading edge of the fins. It should be noted here that all the fins had subsonic leading edges; hence, the difference between the results obtained with the 1-in span and the 2-in.-span fins is not caused by a change from a subsonic to a supersonic leading edge.

To study the effect of span versus chord, Figures 6 and 7 have been included. The effect of varying the span of the fins is shown by the data of Figure 6. One may note a rather sharp increase in magnification factor initially, then a slower increase as the span is increased further. A similar comparison for varying chord with a constant span is displayed in Figure 7. Apparent from Figure 7 is a relatively low value of K for the long (10-in.) fins at low mass flows. This deterioration in complementary reaction force is probably attributable to the low leading edge Mach number, since, under nearly sonic conditions, the high pressures in the separation zone may force flow over the leading edges of the fins quite easily. The experimental data of Figures 6 and 7 have been used to obtain a crossplot of magnification factor, K, versus exposed fin semi-span and fin root chord (Figure 8) for varying chord and varying span, respectively.

In addition to the effect of fin span and chord on the magnification factor there is a dependence of the observed level of interaction upon the circumferential arrangement of the fins. This variation in the reaction force likewise may be attributed to the different patterns of lateral spreading of the

separation zone, resulting from the variant circumferential placements of the fins. This effect is briefly considered in Figure 9, in which data are presented to indicate what happens when the pairs of fins are set at 45°, 90°, or 180° from the orifice position. One observes that the 90° fin arrangement, which restricts the lateral spreading of separation less severely than the 45° fin arrangement, has a lower interaction force than the 45° fin arrangement. The 180° fin arrangement is considered to be the body of revolution without fins. (Refer to Figure 1 for sketch of fin arrangements.)

The effect of angular placement of the fins on the magnification factor, for constant values of the mass flow parameter, may be obtained by crossplotting the data of Figure 9; such a summary plot is given as Figure 10.

The preceding discussion is restricted to the effect of the fins upon the magnitude of the interaction force. In any practical design consideration, however, the fore and aft shift in the center of pressure must be taken into account. Obviously there will be such a shift because the major portion of the interaction force acts at some position in front of the nozzle axis. This forward position of the interaction force is related to the forward progress of the line of separation. A comparison of the separation distance with the forward shift of the center of pressure is provided by the two sets of data assembled in Figure 11. The center of pressure peaks at the point where the separation first passes the apices of the fins. This interpretation of the results appears to be realistic, inasmuch as the high pressures in the separation zone apparently are contained until the separation has spread out ahead of the apices of the fins. The 10-in. fins exhibit retarded progress in the forward movement

of the separation region. This nonuniform rate of advancement seems to stem from the fact that the fins extend past the shoulder of the ogive. Consequently, it turns out that a gradual loss of high pressure apparently occurs as the separation region spills prematurely over the leading edges, rather than around the forward apices of the fins.

The previous discussion has considered the effect of various fin configurations with the same sonic nozzle (d = .172 in.) located symmetrically between the fins. There is, however, an effect of various jet configurations that must be considered. The effect of decreasing the "base" or "escape" area for the separated flow through the addition of fins has been qualitatively discussed previously. It seems possible that the size of this separation "base" area may contribute substantially to the character of the separation. With regard to the three-dimensional aspects of any separation, the separation base area, through which the separated air may escape, is equally as important as the mixing area. Thus, if one can reduce the "base" area, it is possible that the required increase in mixing area will produce a larger separation zone and consequently a larger interaction force.

With this picture of the separation process in mind, various jet arrangements were tested with the 10-in. chord fins (Fin "A"). One, two, or three sonic jets were located symmetrically between a pair of fins, as shown in Figure 1. Thus, as the number of jets located between the fins increased, the separation escape area decreased. The results of these tests are presented in Figure 12. One may note that the slot which spans the entire arc between the fins is the most efficient in producing total normal force. Likewise from Fig-

ure 12 may be seen the relative superiority of the multiple sonic jets over the single sonic jet, in the low mass-flow range except for very weak jets where the experimental inaccuracies increase. As the mass flow increases, however, the efficiency of the multiple sonic nozzles, as compared to the single sonic nozzle, decreases. In the upper range of the mass flows utilized in these tests, the triple sonic nozzles become less efficient than the single sonic nozzle. The reason for this result seems relatively apparent. After the jet configuration has blocked the separation escape area sufficiently to provide maximum interaction force, further increases in jet momentum per unit area result in less normal force for the multiple sonic jets than the single sonic jet because the effective jet thrust in the normal direction becomes less as the nozzles are inclined away from the vertical plane of symmetry. The normal (or measured-interaction-force) direction is defined relative to the horizontal plane of symmetry. This explanation can also be extended to the slot; however, since the slot is a more efficient thrust-producing device than the sonic nozzle, it always maintains relative superiority over the single sonic nozzle. It is also shown in Figure 12 that the double sonic jet configuration follows the same pattern of variation with respect to the single nozzle behavior as the triple sonic jet configuration does, but not to the same quantitative extent, within the range of mass flows examined.

It would seem reasonable to presume that these tests do indicate the importance of blocking the separation escape area with a number of discreet jets or with a slot. The advantages that this blocking may offer in atmospheric flight, however, must be weighed against the loss in efficiency to be antici-

pated for flight outside the atmosphere when circumferential spreading of the nozzles is tantamount to introduction of decreased effectiveness through wasteful misdirection of the jet-reaction vector. Thus the details of the jet configuration must be determined on the basis of the mission characteristics of the vehicle being considered.

The results of the tests of various nozzle arrangements between a pair of fins have been plotted in Figure 13 to show the relative efficiency of the various nozzle-fin configurations. Here once again is shown the superiority of the more efficient slot above all other combinations of sonic nozzles.

Configurations without Fins.--Included in Figure 14 are data to show the relative advantages of supersonic side-jets over sonic side-jets on bodies of revolution without fins. It is seen in Figure 14 that at the larger mass flows the conical nozzles with an exit Mach number of $M_j \doteq 3.0$ are superior (as expected) to sonic nozzles, because of the greater efficiency of the conical nozzles even when exhausting into a vacuum. For comparison, curves are also shown for sonic nozzles on a body with two or four fins.

The results presented in Figure 14 seem to indicate that a substantial increase in total normal force coefficient might be obtained by adding a conical nozzle ($M_j \doteq 3.0$) to a cruciform fin-body configuration. Probably the total normal force coefficient obtained in this manner would be larger than the measured total normal force coefficient found for the sonic-nozzle, cruciform-fin-body configuration, but this deduction has not been verified by an experimental check. It is known[3] that the pressure distributions obtained on a flat plate when a conical nozzle exhausts from the surface of the plate are similar

to those pressure distributions obtained when the conical nozzle is replaced with a sonic nozzle. It is shown later in this report (Figure 17b), however, that the character of the interaction force obtained on a plain body of revolution with a conical nozzle is not the same as the character of the interaction force obtained on the same body with a sonic nozzle. The shapes of conical jets and sonic jets are known to be dissimilar, so that the shape of the shocks ahead of the two different jets may be dissimilar, resulting in pressure distributions, and hence interaction forces, that are not identical. Further experimentation is needed to establish more accurately the nature of interaction flow differences between conical jets and sonic jets.

A correlation of data for the sharp entrance nozzle at various Mach numbers and Reynolds numbers is shown in Figure 15. This correlation seems to indicate that the interaction force obtained when a jet nozzle exhausts from the side of a body of revolution immersed in a supersonic stream is relatively insensitive to Reynolds number variation, at least within the range of Reynolds numbers covered in this report, where the boundary layer remained laminar. The effect of an artifical trip in causing the boundary to become turbulent and significantly altering the separation phenomena ahead of the jet will be discussed later.

The main results of the body-without-fins experiments are collected together in Figure 16. Impulse versus the reciprocal of total normal force coefficient is shown in Figure 16a, while impulse versus the reciprocal of the mass flow parameter is given in Figure 16b. The superiority of conical nozzles to the sonic nozzles, in the high range of total normal force coefficient and

mass flow, is evident from Figure 16, but as the normal force or mass flow decreases, the sonic nozzles become superior to the conical nozzles. This result occurs even though the conical nozzles produce more direct thrust than sonic nozzles, because larger interaction forces are obtained with sonic nozzles in the low-mass-flow range. The same result was observed in Ref. 3 for a flat plate. A calculation made subsequent to publication of Ref. 3 showed that this relative inferiority of conical nozzles in the low-thrust range cannot be attributed to flow separation within the nozzle. Here in Figure 16 the results once again indicate that interaction phenomena, produced when sonic nozzles exhaust from a body of revolution without fins into a supersonic main stream, are substantially different from the interactions produced when the sonic nozzles are replaced by conical nozzles.

The sharp-entrance nozzle is an inefficient nozzle when its characteristics are compared to the calculated characteristics of an ideal sonic nozzle and even when compared experimentally under vacuum-exhaust conditions with the sonic nozzles used in these tests. As shown in Figure 16, however, the sharp-entrance nozzle produces more interaction impulse, within the range of mass flows measured, than the sonic nozzles. Separation occurring inside the sharp-entrance nozzle reduces the effective throat area of the nozzle and makes it a psuedo-bell-shaped nozzle. This effective change in throat contour implies that the exit Mach number for the sharp-entrance nozzle will be somewhat greater than the Mach number attained at the exit of the sonic nozzle. Furthermore, the radical alteration in character of the flow at the nozzle exit means that the shape of the jet issuing from the sharp-entrance nozzle is somewhat different from the

shape of a sonic jet, although the amount of this difference is not known in any precise detail at this time. Thus the jet from the sharp-entrance nozzle, while producing apparently the same trends as a sonic jet, generates total forces and interaction forces of slightly greater magnitude than those for sonic jets for the same jet mass-flow.

The group of experimental findings presented in Figure 17a shows that the magnification factor obtained on a body of revolution without fins decreases as the distance from the nozzle centerline to the body base (afterbody length X') increases. (When the afterbody length X' is increased, the value of L/X increases slightly.) This change in magnification factor appears to be a result of high pressures in the separated zone propagating around the body (without fins), to envelop a fairly large area of the body opposite the jet. Behind the jet there is a low-pressure area similar to that found behind any obstructing body in a supersonic stream. Thus the relatively high (compared to free-stream) pressure on the underside of the body and the relatively low pressure on the top side of the body behind the jet contribute to formation of a net force which tends to counteract the jet thrust. The result is a net decrease in the total normal force. This general behavior was also recognized in earlier unpublished data obtained for a side jet exhausting from a cone-cylinder body of revolution at $M_\infty = 2.84$.

In Figure 17b one can see the difference in the character of the interaction-force curve obtained when a sonic nozzle is replaced by a conical nozzle. Whereas the interaction forces produced by the sonic jets employed in the present set of experiments varied by about 70% over the range of mass flows measured,

the interaction forces produced by the conical jets vary only about 20%, over approximately the same range of mass flows. A conical jet is an inferior interaction-force producer in the low mass-flow range and only slightly superior to a sonic jet in the high mass-flow range. One is led to the obvious conclusion, from scrutiny of the data presented in Figure 17b, that the interaction phenomena produced by conical jets is different from the interaction phenomena produced by sonic jets.

If the boundary layer on the body is changed from laminar to turbulent, the interaction force and thus the total normal force is increased by approximately 10% in the high range of jet mass flows as is shown in Figure 17b. This result was obtained with a sharp entrance nozzle, the boundary layer being tripped from laminar to turbulent by installation of an "O" ring on the nose of the model. It is believed that the same approximate result would be obtained if the nozzle tested were a sonic nozzle instead of the sharp-entrance nozzle actually used, because, as mentioned previously, the trends established by the two nozzles are quite similar.

A comparison of magnification factors for the long and the short test bodies can be seen in Figure 17b. The increased interaction forces on the long body may be due to different boundary layer characteristics at the nozzle centerline which result from the increased distance of the jet from the ogive cylinder junction.

The interaction forces plotted in Figure 17 are replotted in Figure 18 by resort to a slightly different parameter. By using this pressure-ratio to diameter-ratio parameter, it was found possible to correlate previously ob-

tained data given in Ref. 3 pertaining to a similar body of revolution. The data from the present tests are plotted in Figure 18a and then compared in Figure 18b, with the data from Ref. 3. In this manner it may be seen that there is good correspondence between the results of this test program and the results presented in Ref. 3.

Side-jet reaction controls located near the nose of a missile are of interest for some applications. Consequently, a limited amount of exploratory testing of a nose-mounted-nozzle configuration was conducted. The results of such preliminary testing are presented in Figure 19. The nozzle in the nose of the body of revolution is a sharp-entrance nozzle 0.160 in. in diameter. To assure parity in the test conditions, comparison is made in Figure 19 with the results obtained for an aft-situated nozzle having the same variety of sharp entrance. It is seen that mounting the nozzle in the nose of the body seriously decreases its over-all efficiency. Possibly this deterioration in effectiveness is ascribable to the fact that when the jet is close to the nose of the body there is very little area over which the high pressures in the separation zone can act, while there is an extensive area behind the jet over which the low pressures in the jet wake can act, to result in production of a net negative interaction force, as shown in Figure 19.

The variation of the location of the center of pressure of the total normal force, with change in the mass flow, for the various nozzle configurations tested on a body of revolution without fins, is presented in Figure 20. Again one can see a marked difference between the performance of sonic and conical nozzles for a body of revolution without fins. In the low range of jet mass flows,

where the interaction force for the sonic jets was higher than the interaction force for the conical jets, the center of pressure of the total normal force is further ahead of the nozzle centerline for the sonic jets than for the conical jets. It is evident, besides, that there is a distinct increase in the forward movement of the center of pressure of the total normal force for sonic jets with increase in afterbody length. This integrated result arises chiefly because the negative interaction force, located behind the jet, is increased with increasing afterbody length. It has been shown earlier that the total normal force produced by a given nozzle is independent of Reynolds number, if no transition to turbulent flow occurs ahead of the separation point. As the afterbody length is increased, therefore, the net interaction force produced by the high pressures in the separation region ahead of the nozzle centerline should remain relatively constant, for a given jet mass flow. The moment produced by this net interaction force acting ahead of the jet will also remain relatively constant. Thus when a negative interaction force is exerted near the rear of the body, the apparent point of application of the resultant total normal force must move upstream. This concept of the play of forces involved is confirmed by the result shown in Figure 20.

The magnitude of the interaction force obtained for a given nozzle geometry and mass flow was seen (Figure 17b) to be greater when the boundary layer was turbulent than when it was laminar. In Figure 20, it is seen that the character of the variation of center of pressure location also is different between turbulent and laminar boundary layers. When the boundary layer is laminar, the high pressures in the separation zone can separate the boundary

layer quite easily, hence the separation zone is quite large. When the boundary layer becomes turbulent, however, the high pressures within the separated zone are confined to a smaller area by action of turbulent transport in retarding the spread of separation. As a result of this confinement, the center of pressure cannot move as far upstream as it does when the boundary layer is laminar.

A comparison is made in Figure 21 between the results of Ref. 3, for a flat plate, with the results presented herein for the body of revolution with and without fins. It is seen in Figure 21 that the magnitude of the interaction force obtained on the body of revolution with the cruciform fins compares favorably with the flat plate data, while all other body-of-revolution configurations exhibit interaction forces of lesser magnitude.

A confrontation is presented in Figure 22, at a free-stream Mach number, $M_\infty = 4.0$, between two existing side-jet interaction theories and between empirical predictions and experimental results. The Amick theory[2] is a simple two-dimensional theory that includes viscous effects. The Ferrari theory[7] is more comprehensive, but it is limited to inviscid hypersonic flows. The magnitude of the interaction force predicted by these two theories at $M_\infty = 4.0$ is approximately the same in this instance, but this particularly close agreement is considered to be only a coincidence. At higher Mach numbers the correlation between these theories is not as good. Both theories appear to over-emphasize the interaction forces produced on bodies of revolution without fins at $M_\infty = 4.0$.

In Ref. 2 an empirical equation was presented for predicting the interaction forces on bodies of revolution at $M_\infty = 2.84$. This equation, which fits the experimental data well at $M_\infty = 2.84$, is also shown in Ref. 2 to be able to predict

fairly well the interaction forces obtained at $M_{\infty} = 3.90$ when the boundary layer is turbulent. A comparison is given, in addition, in Figure 22 between the predictions based on use of this empirical equation of Ref. 2 and experimental data obtained at $M_{\infty} = 3.97$, with a turbulent boundary layer, This empirical equation apparently has a limited range of applicability, but its usefulness in the restricted range for which it was designed cannot be denied.

CONCLUSIONS

A study has been conducted of the effects of exhausting a side-jet nozzle normal to the surface of a body of revolution, with and without fins, immersed in a supersonic stream. From this study it is concluded that:

1. A beneficial interaction force may be obtained from the side-jet, supersonic-stream interaction.

2. The magnitude of the interaction force is much greater on a body of revolution with fins than on a body of revolution without fins.

3. The magnitude of the interaction force is dependent upon side-jet nozzle geometry.

4. For the body of revolution without fins, the magnitude of the interaction force obtained decreases as the nozzle moves forward on the body, becoming negative for far forward nose locations.

5. The interaction forces obtained on a body of revolution without fins when the boundary layer is turbulent exceed the interaction forces obtained on the body when the boundary layer is laminar for high values of jet mass flow.

6. Existing theories do not adequately predict the magnitude of the interaction force on bodies of revolution without fins.

REFERENCES

1. Morkovin, M.F., Pierce, D.A. Jr., and Craven, C.E., Interaction of a Side-Jet with a Supersonic Main Stream, University of Michigan Engineering Research Institute, Bulletin No. 35, Sept., 1952.

2. Vinson, P.W., Amick, J.L., and Liepman, H.P., Interaction Effects Produced by Jet Exhausting Laterally Near Base of Ogive-Cylinder Model in Supersonic Main Stream, NASA Memo 12-5-58W, Feb., 1959.

3. Amick, J.L., Hays, P.B., Interaction Effects of Side Jets Issuing from Flat Plates and Cylinders Alined with a Supersonic Stream, Wright Air Development Division, TR 60-329, May, 1960.

4. Liepman, H.P., Amick, J.L., and Reynolds, T.H., Calibration Report on The University of Michigan 8-by 13-inch Supersonic Wind Tunnel, Part V, Aerodynamic Calibration at Nominal Mach Number of 2.43, WTM-248, The University of Michigan Engineering Research Institute, Jan., 1954.

5. Carvalho, G.F., Calibration Report on The University of Michigan 8- by 13-inch Supersonic Wind Tunnel, Calibration at Nominal Mach Number of 3.90, WTM-268, The University of Michigan Research Institute, March, 1960.

6. "Supplement to ASME Power Test Codes, Part 5- Measurement of Quantity of Materials, Chapter 4- Flow Measurements," New York, American Society of Mechanical Engineers (1959).

7. Ferrari, C., Interference Between a Jet Issuing Laterally from a Body and the Enveloping Supersonic Stream, Johns Hopkins University, Applied Physics Laboratory Report No. 286, Section T, April, 1959.

APPENDIX

Tests were conducted in a tank that was maintained at a pressure of approximately 2 mm Hg absolute to determine the thrust and mass flow characteristic of the nozzles used during these experiments. Supplementary tests have shown that any error that might arise in the measurement of the jet thrust because of flow induced over the body by the jet is negligible at this low pressure. Jet-thrust and mass-flow curves for all nozzles tested, except for the nozzle in the nose of the long-model forebody, are included in Figures 23 and 24.

The jet-thrust curves as presented in Figure 24a reveal the apparent inefficiency of the sharp-entrance nozzle. By the use of the china-clay technique, it was discovered that the flow in the sharp-entrance nozzle was separated. The flow separated at the nozzle entrance and re-attached to the nozzle wall just ahead of the nozzle exit. Thus, in reality, the effective nozzle-throat diameter for this configuration was always less than the geometric diameter of 0.160 in.

Differences may be detected in Figure 24a between the performances exhibited by the several sonic nozzles, as exemplified in the jet-thrust curves. Although the sonic nozzles were geometrically similar, the model internal geometry for the various nozzle configurations was different for each sonic nozzle. Therefore, because of the different internal-flow conditions for each sonic nozzle, the differences noted in the jet-thrust curves are not unexpected.

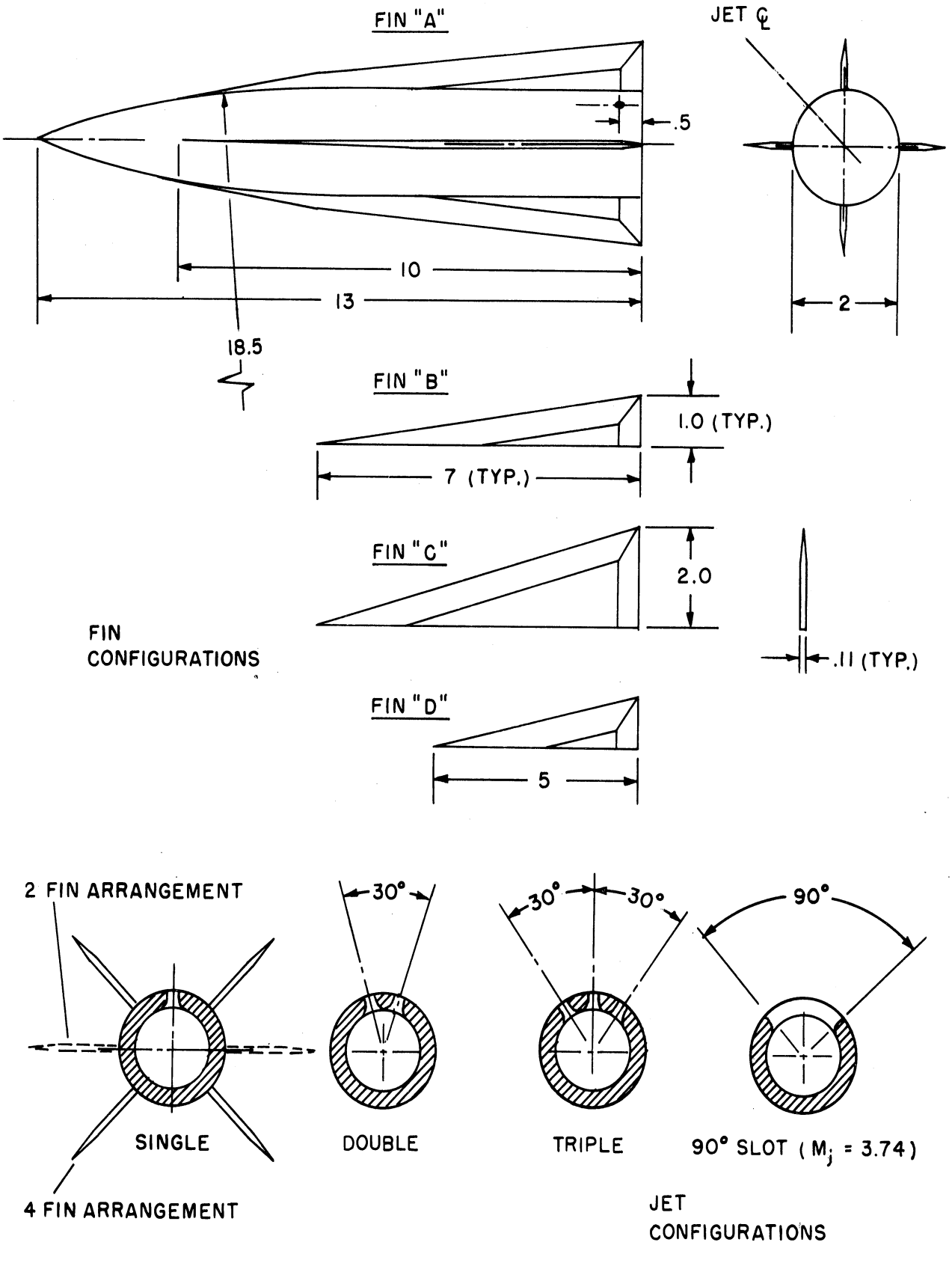

FIGURE 1. LONG MODEL: NOZZLE AND BODY OF REVOLUTION WITH FINS; SHOWN 1/3 ACTUAL SIZE.

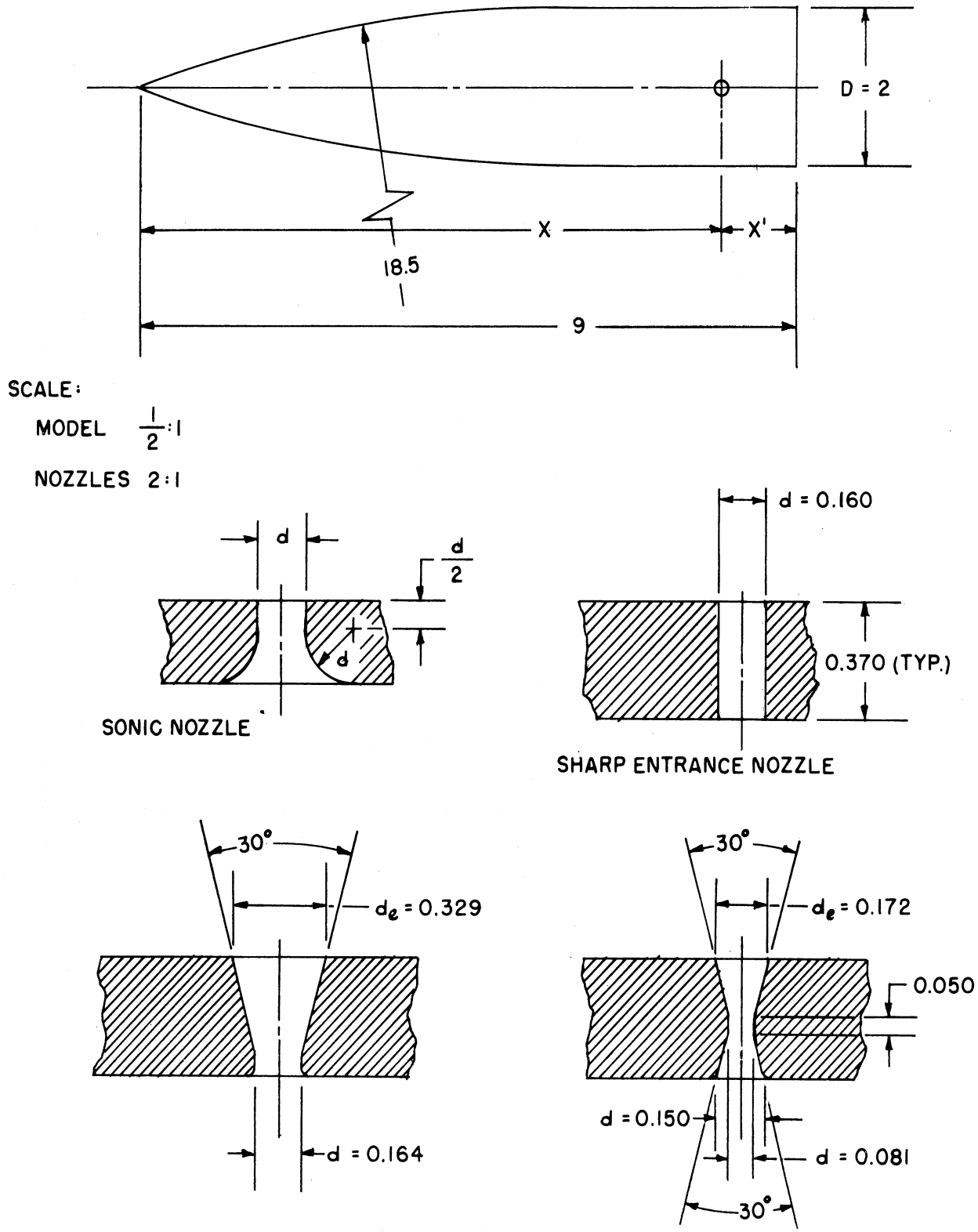

FIGURE 2. SHORT MODEL: NOZZLE AND BODY OF REVOLUTION WITHOUT FINS.

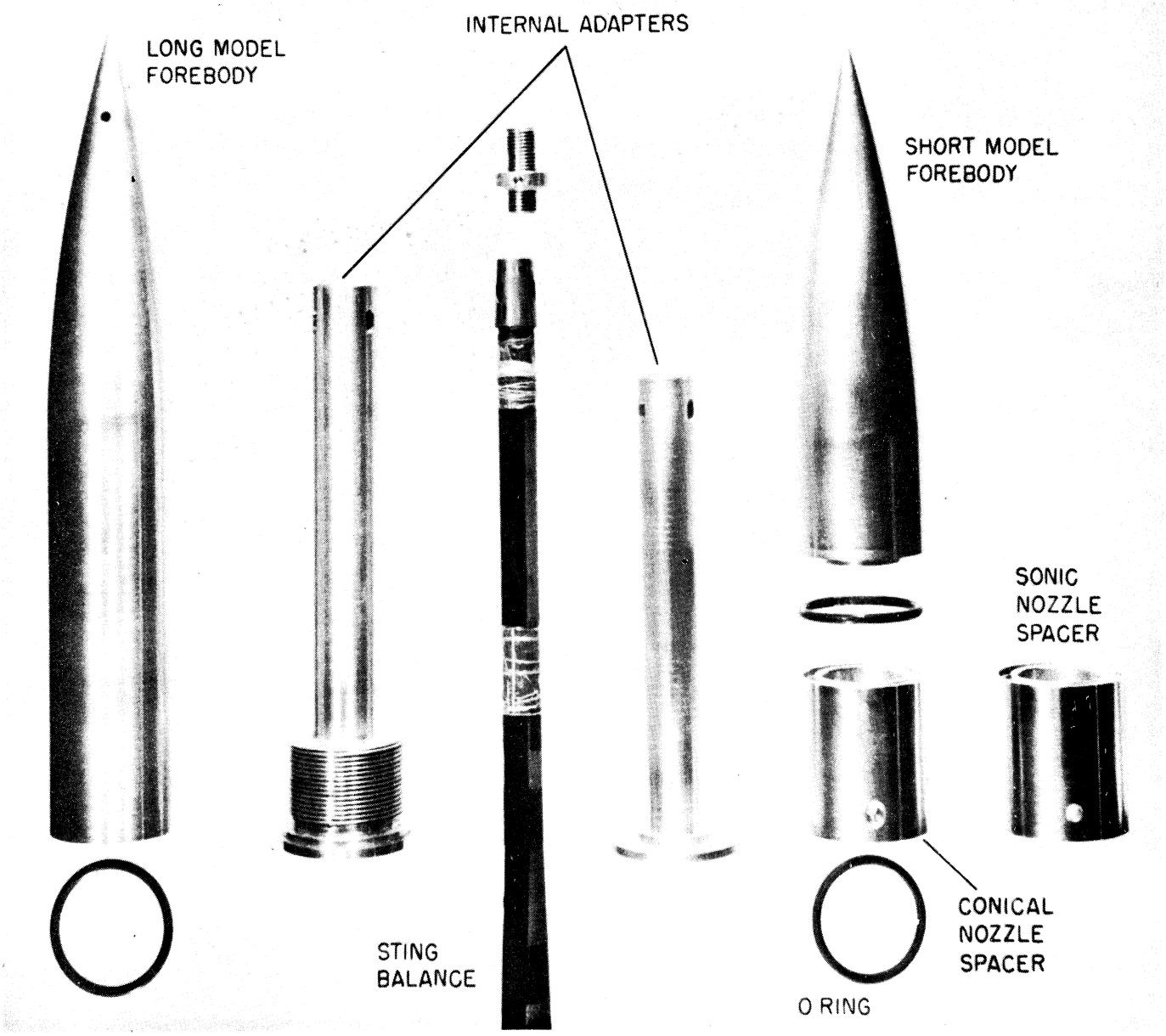

FIGURE 3. LONG AND SHORT MODEL FOREBODIES, STING BALANCE AND TWO NOZZLE SPACERS.

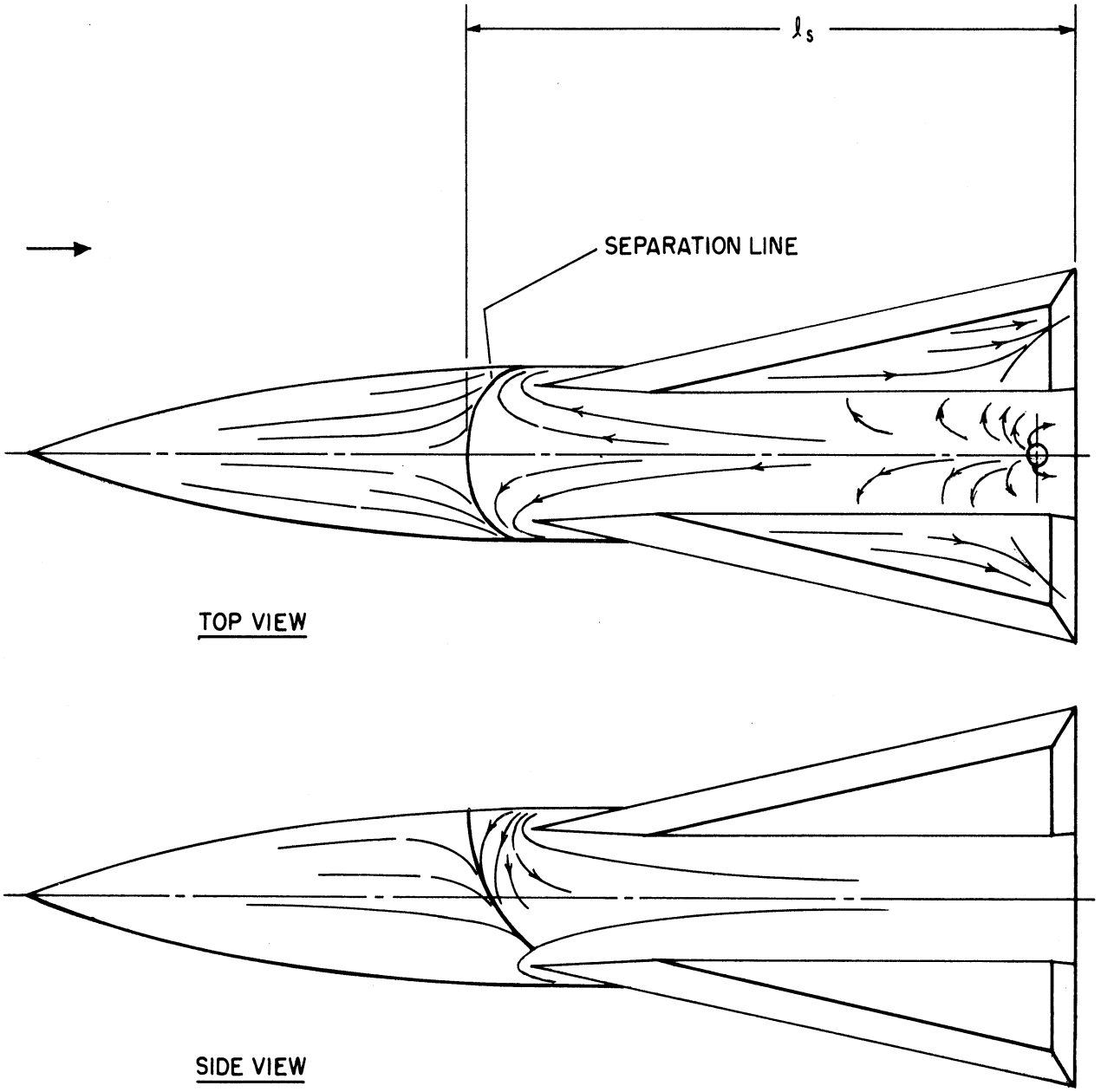

(a) BODY OF REVOLUTION WITH FINS

FIGURE 4. SKETCHES OF TYPICAL CHINA CLAY PATTERNS.

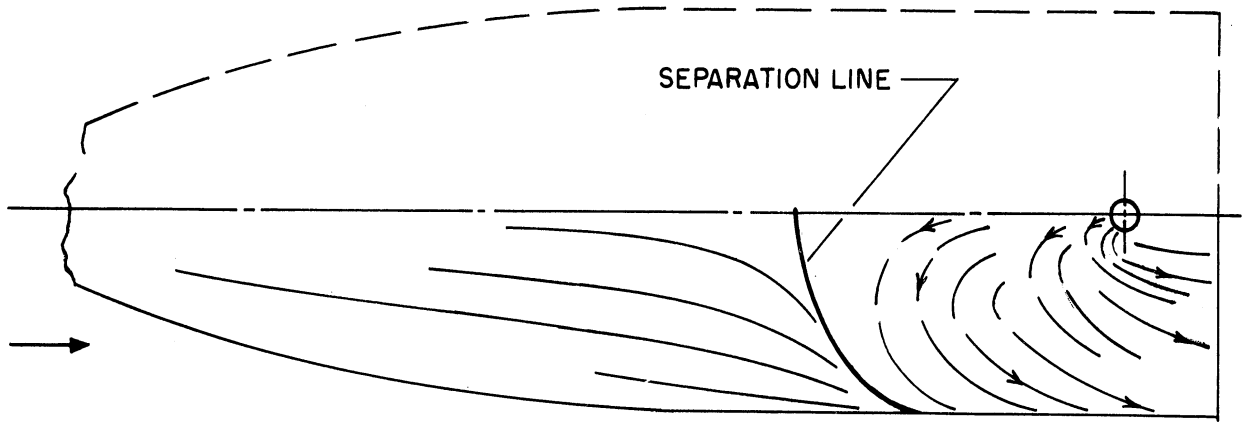

TOP VIEW

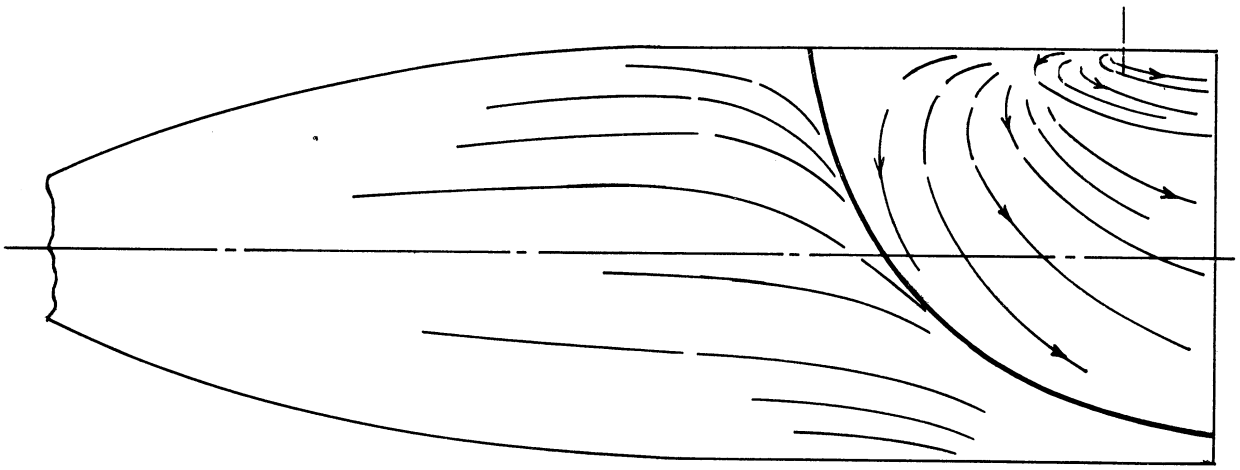

SIDE VIEW

(b) BODY OF REVOLUTION WITHOUT FINS

FIGURE 4. CONCLUDED.

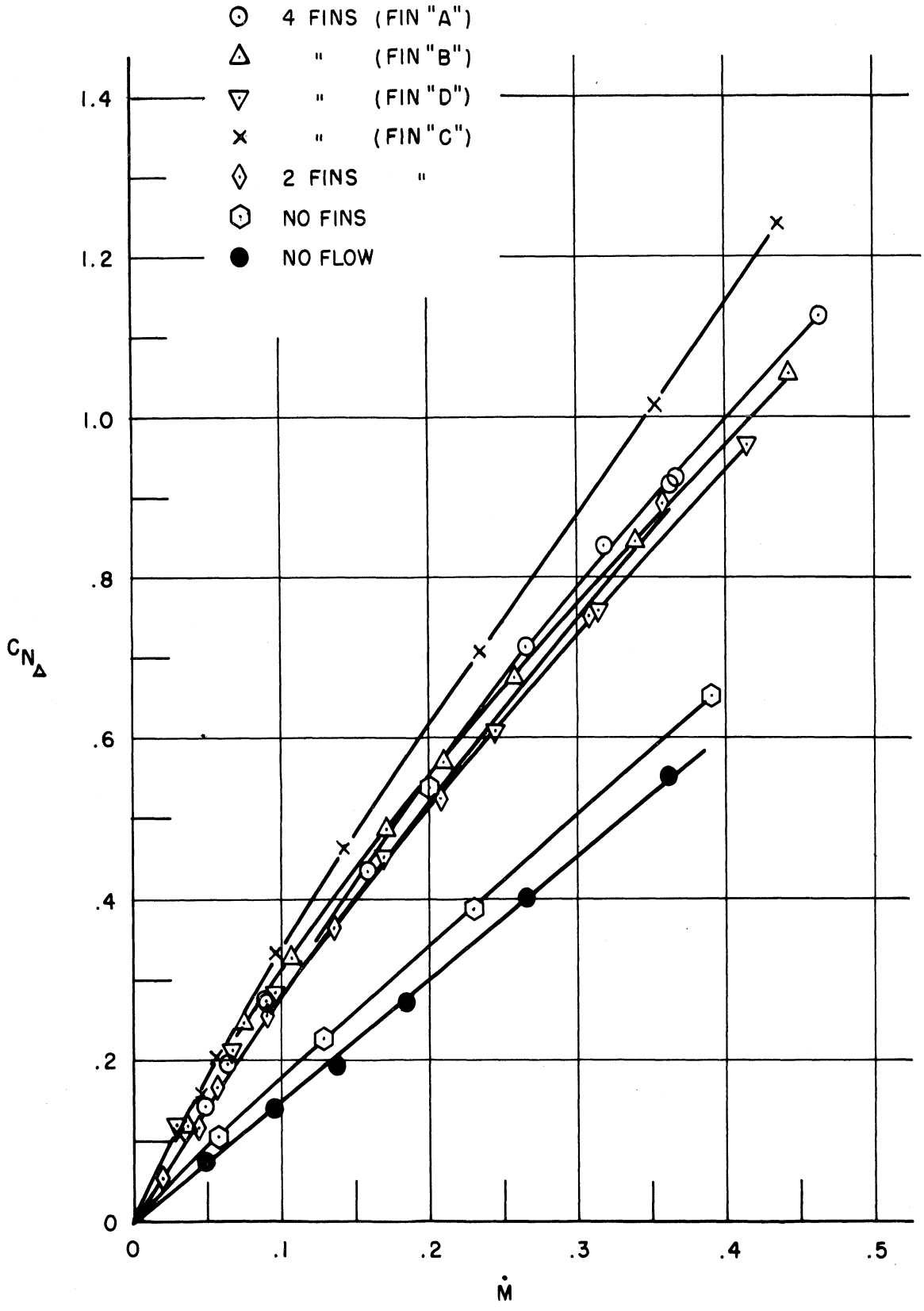

FIGURE 5. VARIATION OF INTERACTION FORCE WITH MASS FLOW PARAMETER FOR SEVERAL FIN-BODY CONFIGURATIONS; $M_\infty = 3.97$, SONIC NOZZLE, $d = 0.172$.

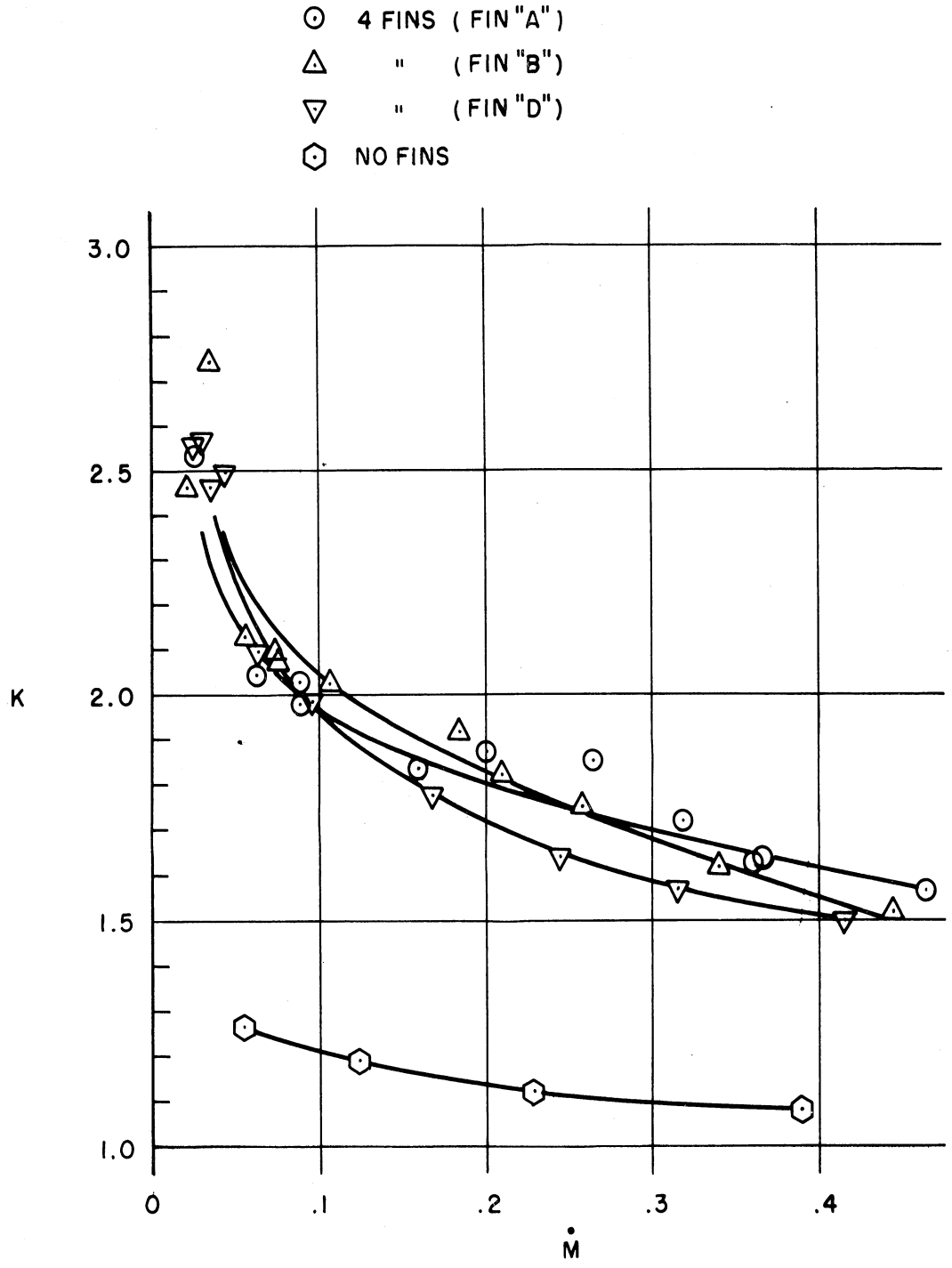

FIGURE 7. MAGNIFICATION FACTOR VARIATION WITH MASS FLOW PARAMETER FOR VARIOUS FINS OF CONSTANT SPAN ;
M_∞ = 3.97, SONIC NOZZLE, d = 0.172, b = 1.0 .

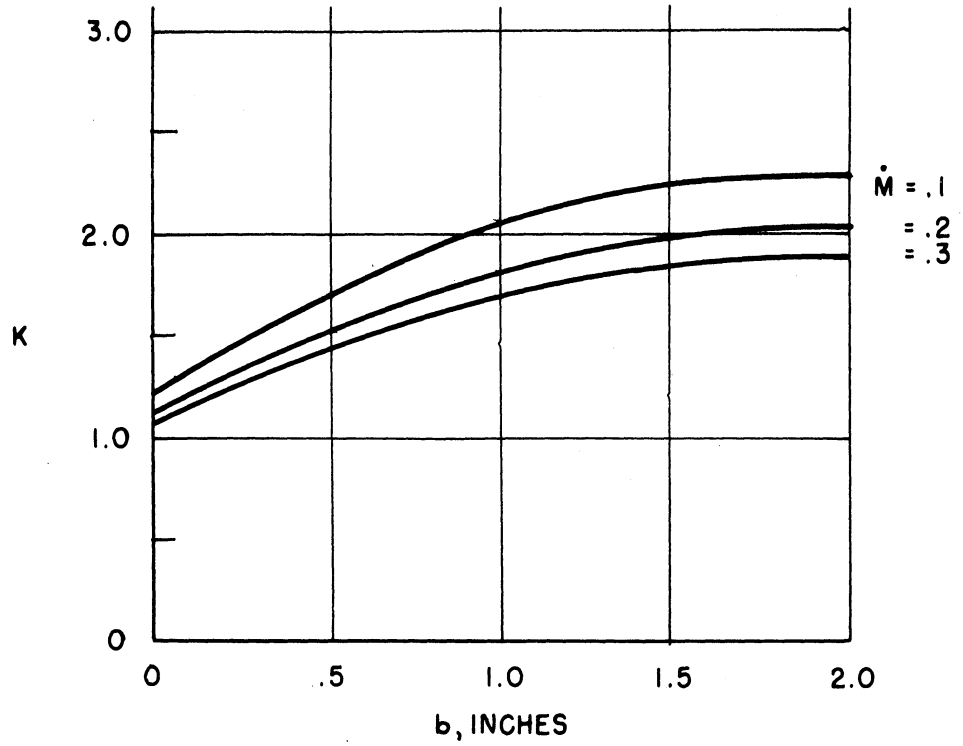

(a) CONSTANT CHORD = 7.0

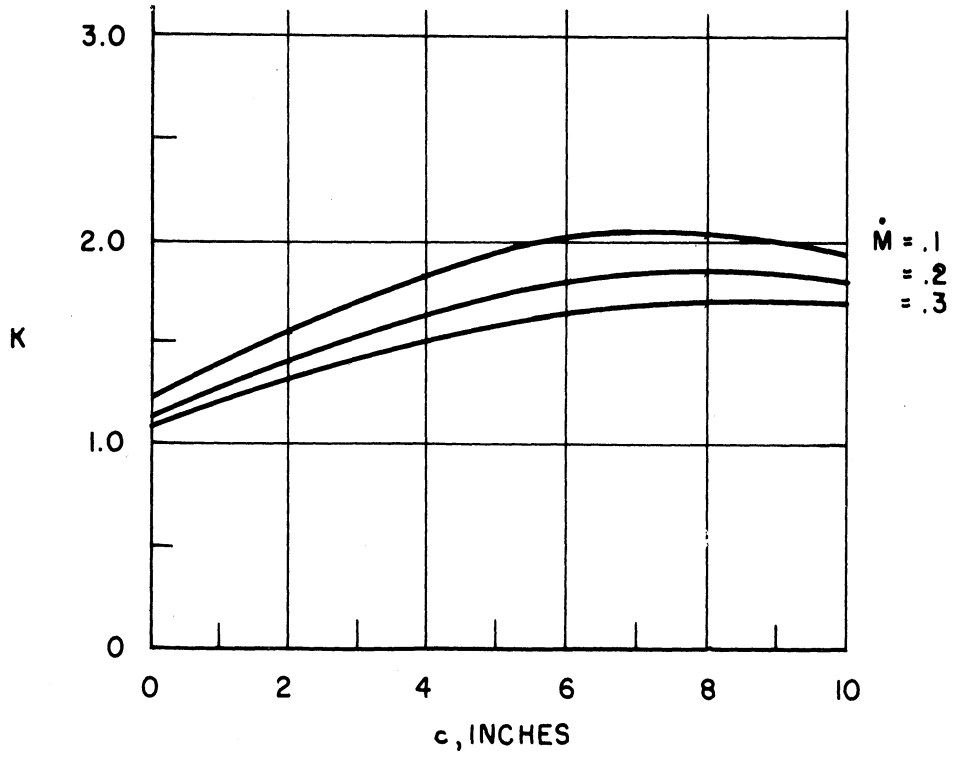

(b) CONSTANT SPAN = 1.0

FIGURE 8. MAGNIFICATION FACTOR FOR CONSTANT CHORD AND CONSTANT SPAN FINS: M = 3.97, d = 0.172 .

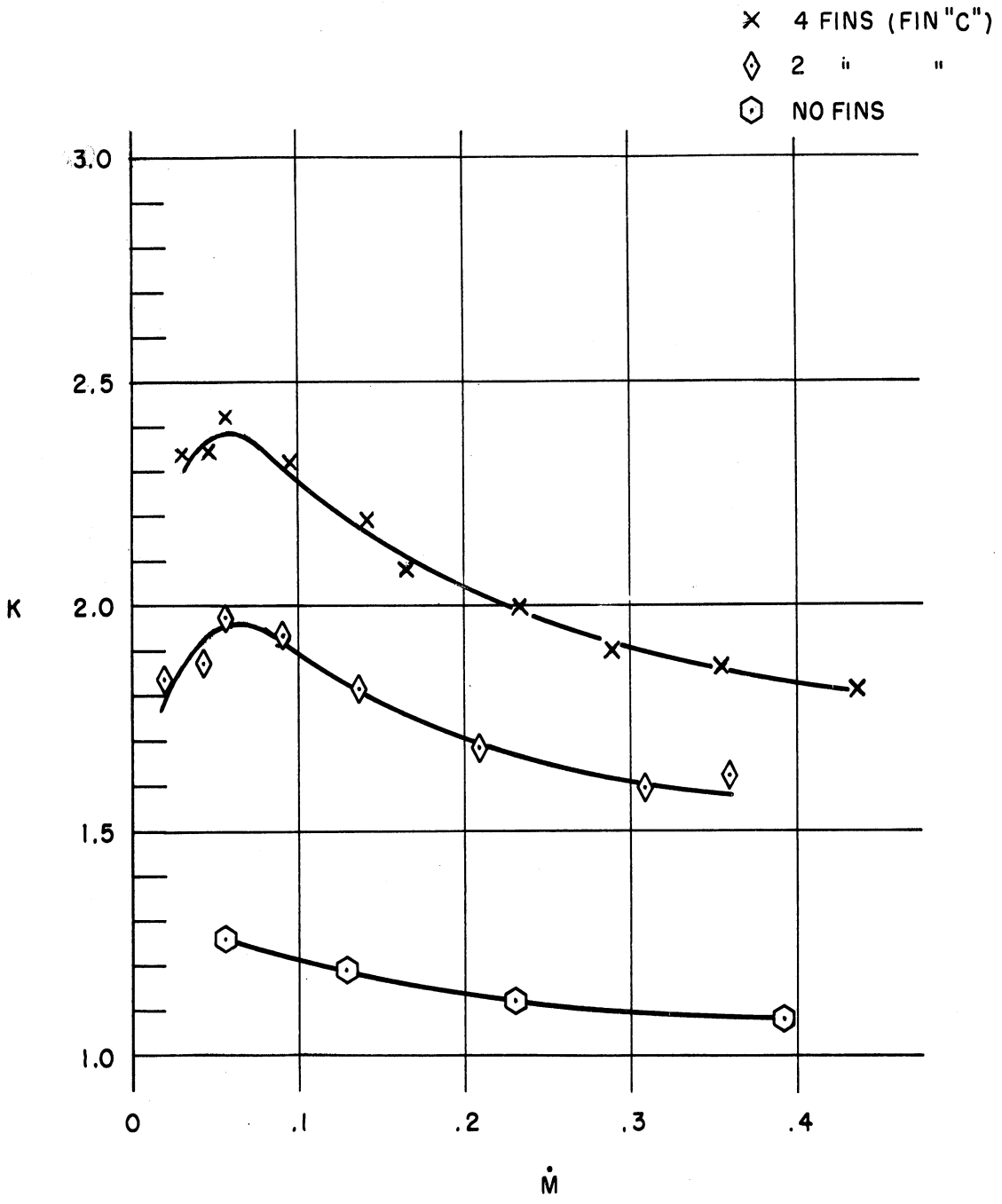

FIGURE 9. MAGNIFICATION FACTOR VARIATION WITH MASS FLOW PARAMETER FOR VARIOUS CIRCUMFERENTIAL FIN ARRANGEMENTS; $M_\infty = 3.97$, SONIC NOZZLE, $d = 0.172$.

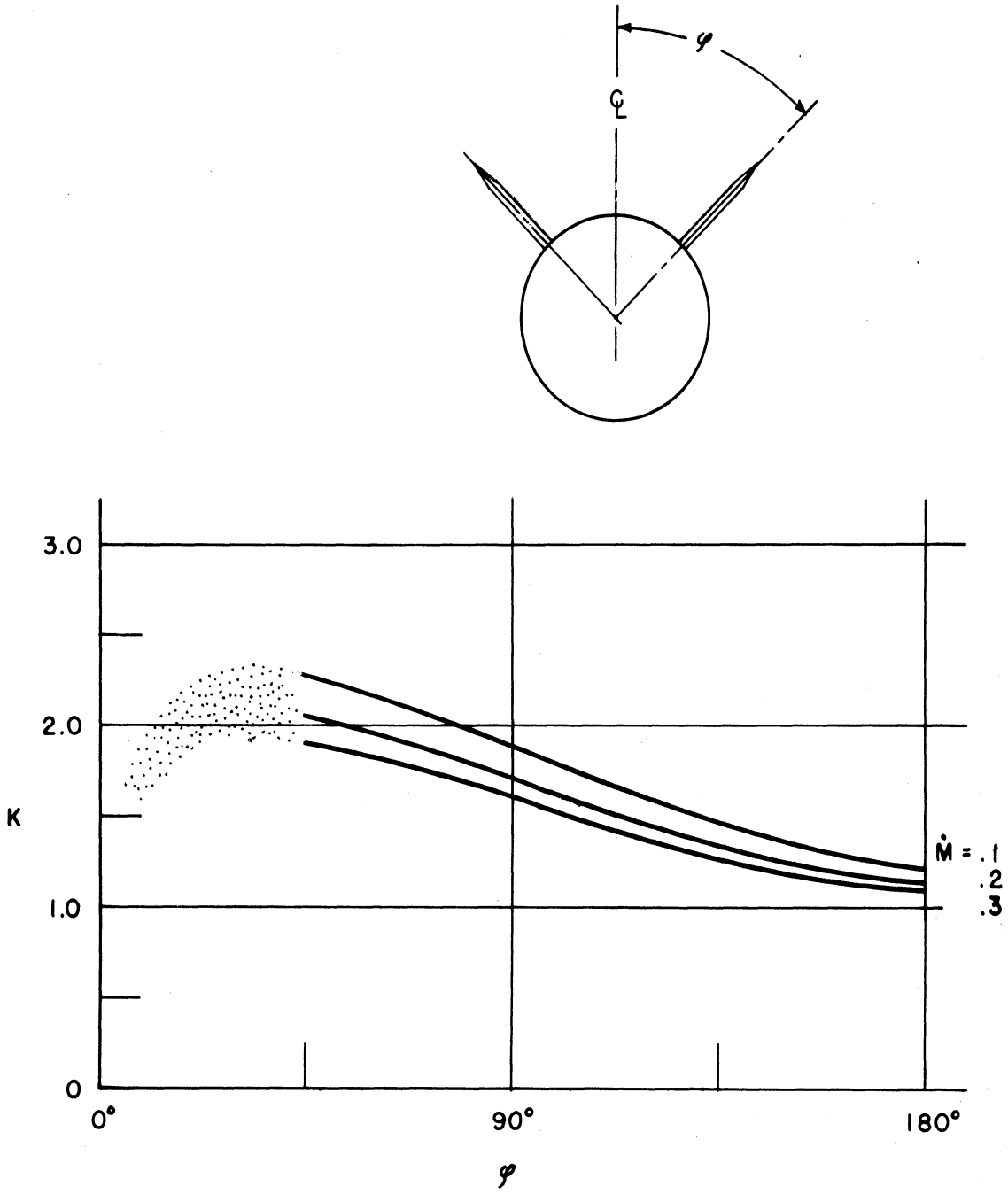

FIGURE 10. MAGNIFICATION FACTOR VARIATION WITH MASS FLOW PARAMETER FOR VARIOUS CIRCUMFERENTIAL FIN POSITIONS; $M_\infty = 3.97$, SONIC NOZZLE, $d = 0.172$, FIN "C".

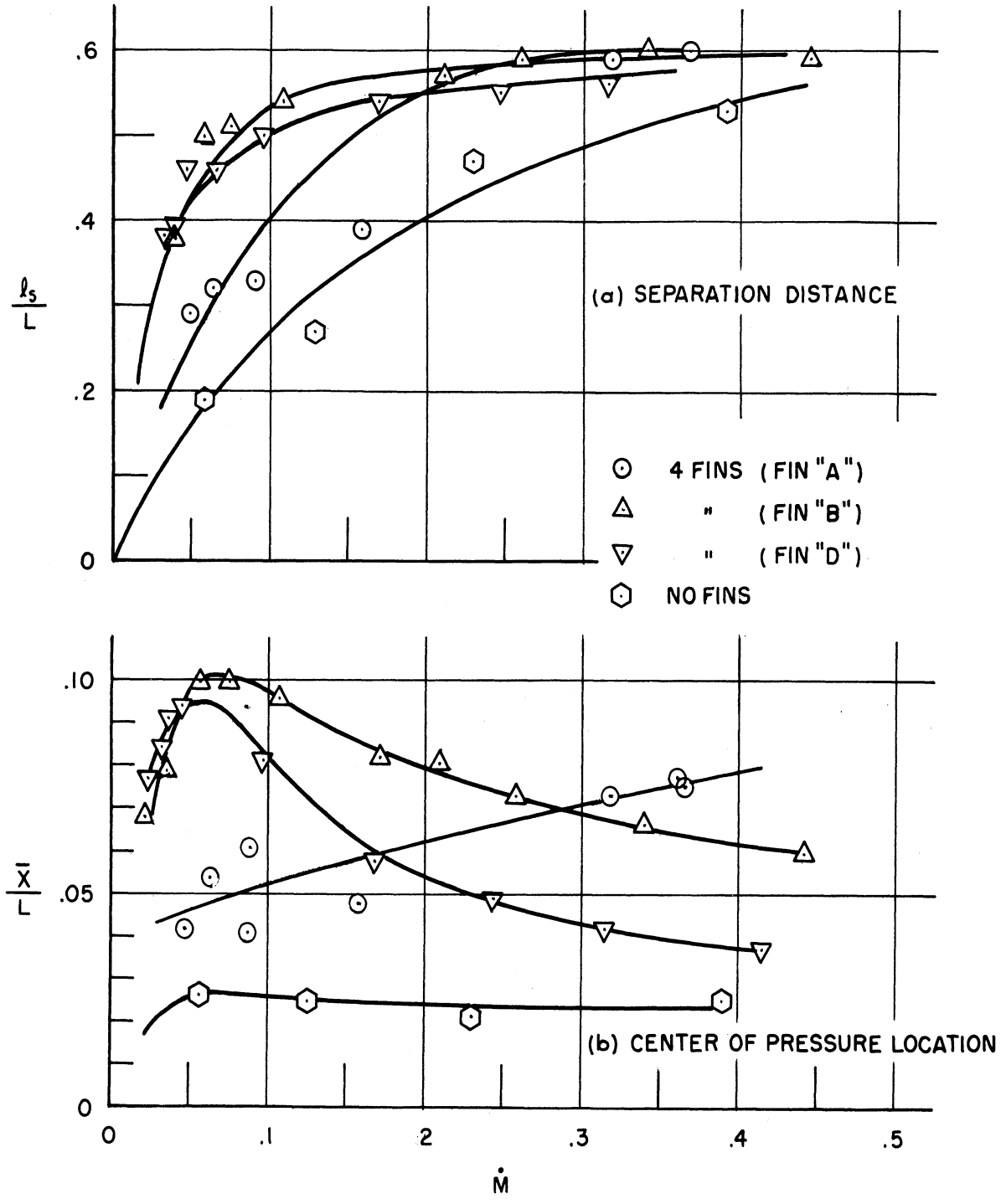

FIGURE 11. CENTER OF PRESSURE AND STREAMWISE SEPARATION DISTANCE VARIATION WITH MASS FLOW PARAMETER FOR VARIOUS FINS WITH CONSTANT SPAN; $M_\infty = 3.97$, SONIC NOZZLE, $d = 0.172$.

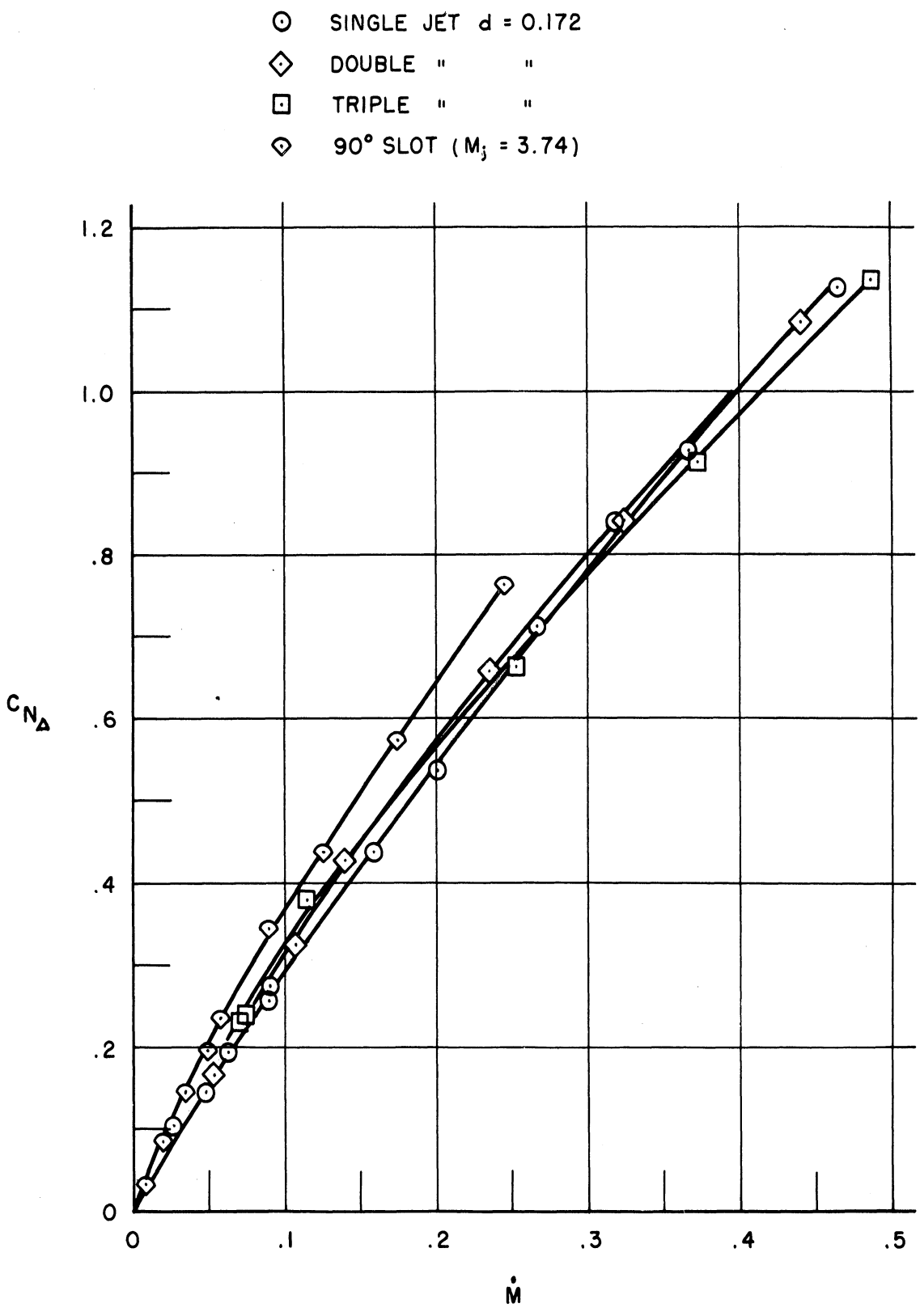

FIGURE 12. TOTAL NORMAL FORCE COEFFICIENT VARIATION WITH MASS FLOW PARAMETER FOR VARIOUS NOZZLE-FIN COMBINATIONS; M_∞ = 3.97, FIN "A", 4 FINS.

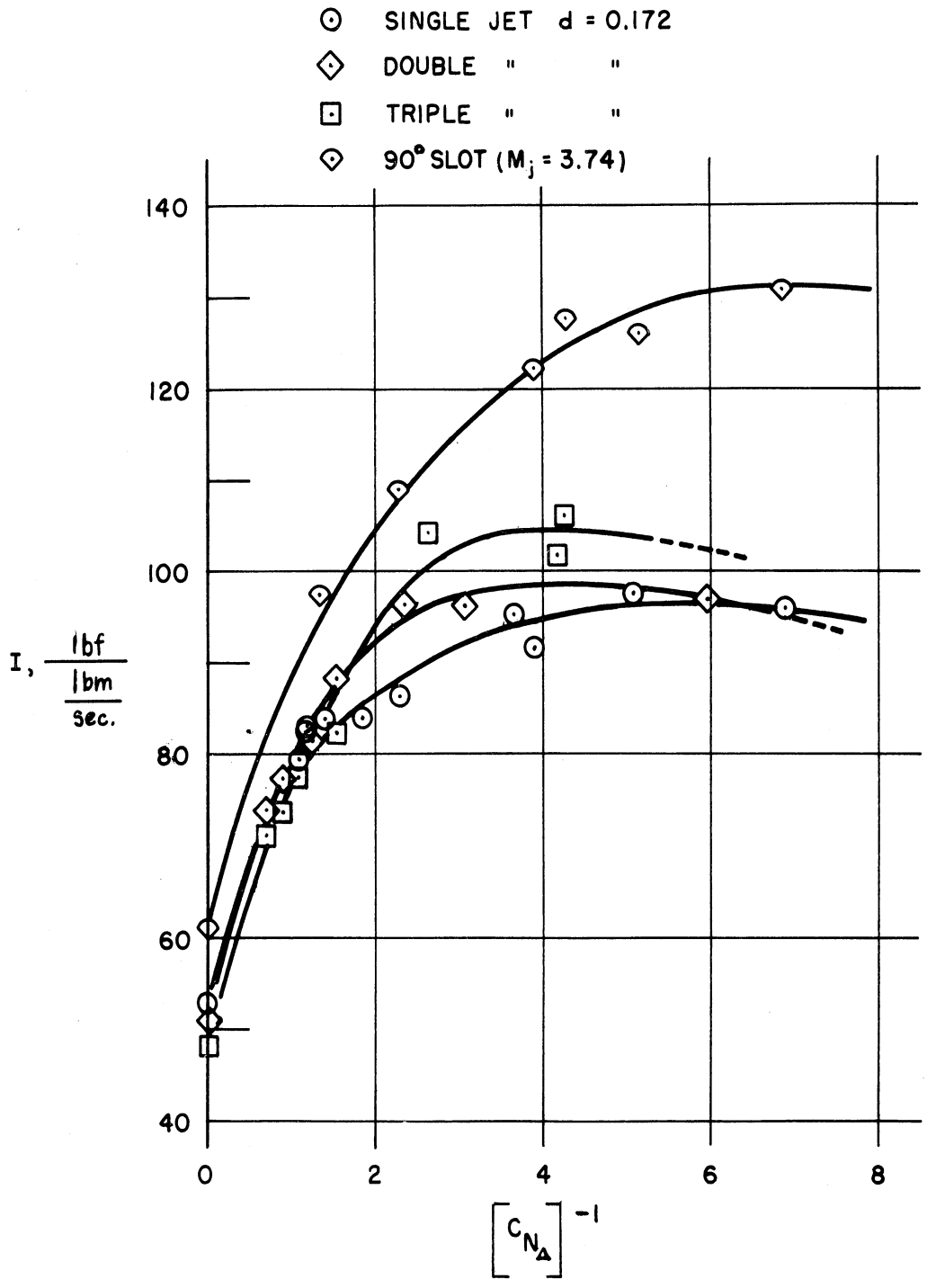

FIGURE 13. IMPULSE VARIATION WITH TOTAL NORMAL FORCE COEFFICIENT FOR VARIOUS NOZZLE-FIN COMBINATIONS; M_∞ = 3.97, FIN "A", 4 FINS.

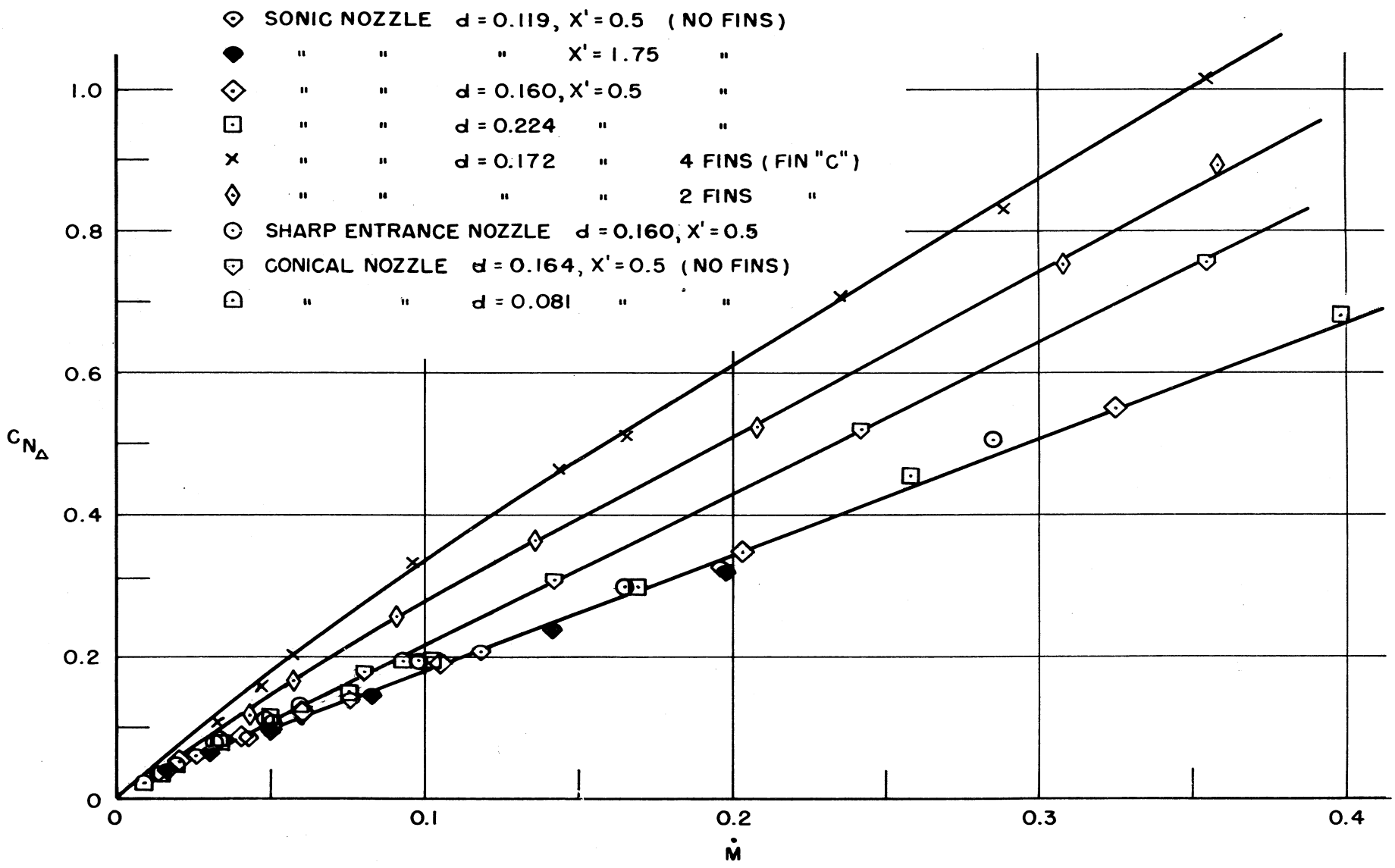

FIGURE 14. VARIATION OF TOTAL NORMAL FORCE COEFFICIENT WITH MASS FLOW PARAMETER FOR VARIOUS NOZZLE GEOMETRIES, AFTERBODY LENGTHS AND FIN CONFIGURATIONS; $M_\infty = 3.97$, $L = 9.0$.

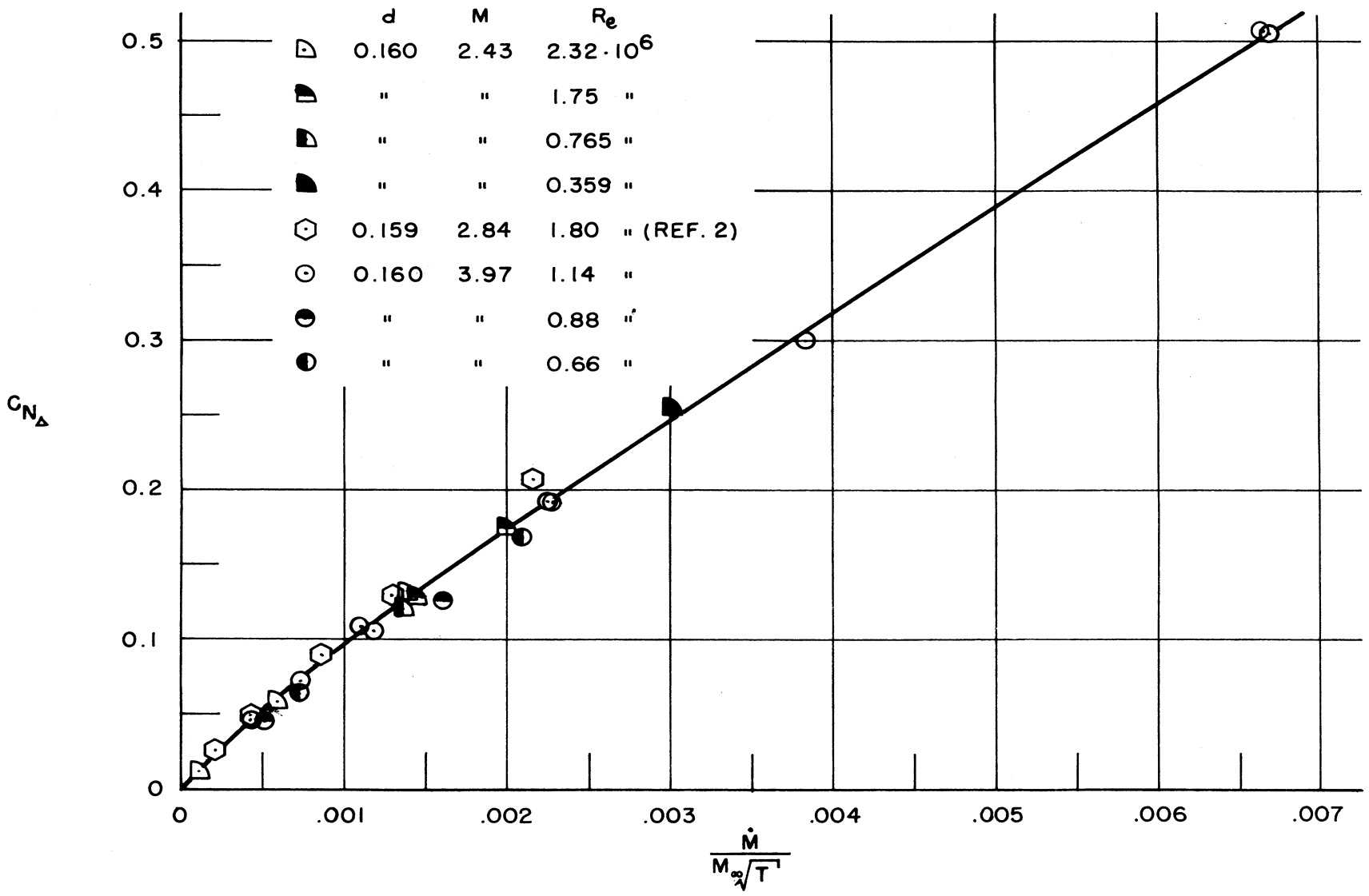

FIGURE 15. CORRELATION OF TOTAL NORMAL FORCE COEFFICIENTS FOR VARIOUS MACH NUMBERS AND REYNOLDS NUMBERS; X = 8.50, L = 9.0, NO FINS, SHARP ENTRANCE NOZZLE.

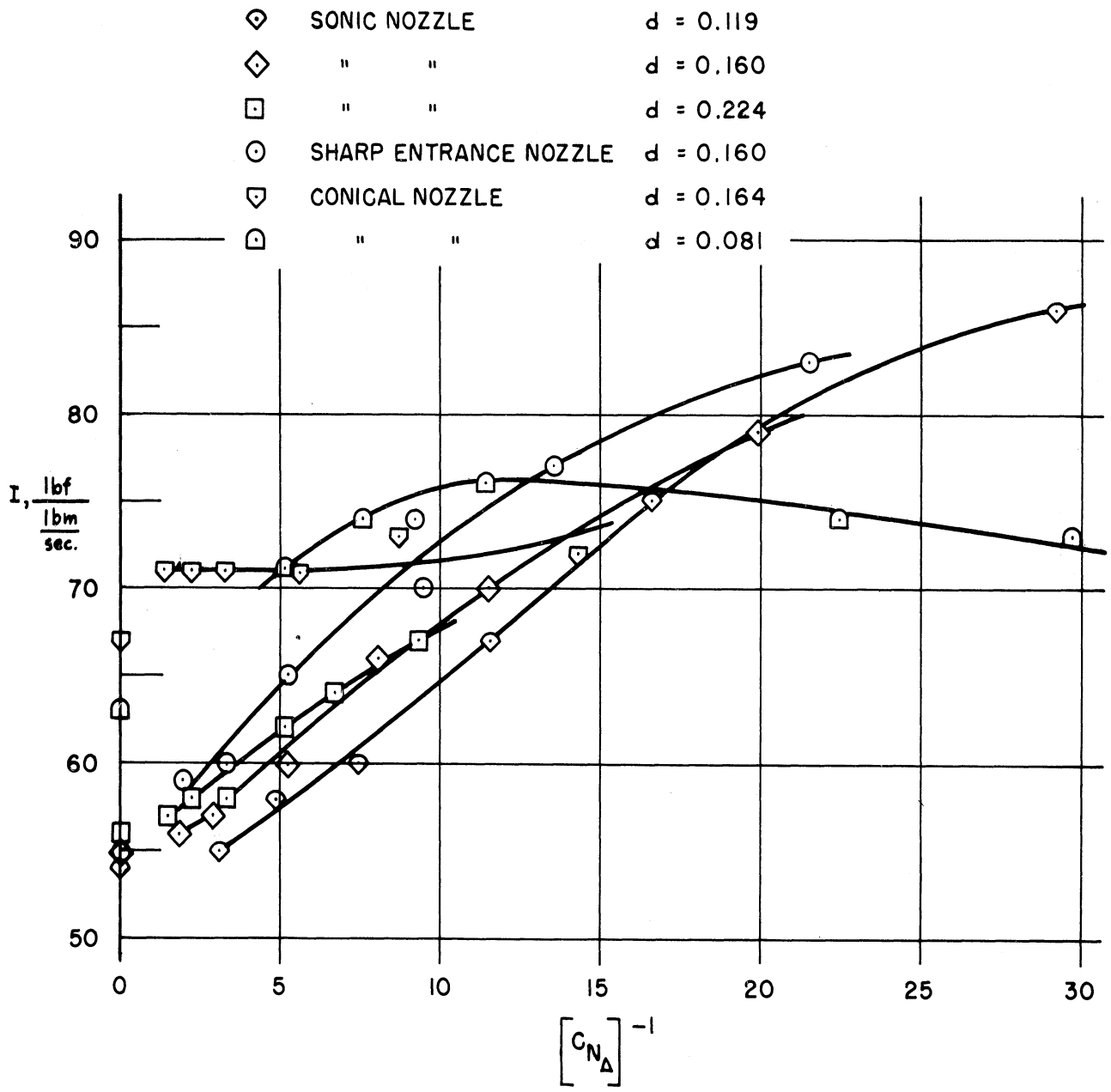

(a) IMPULSE VARIATION WITH TOTAL NORMAL FORCE COEFFICIENT.

FIGURE 16. IMPULSE VARIATION WITH TOTAL NORMAL FORCE COEFFICIENT AND MASS FLOW PARAMETER FOR VARIOUS NOZZLE GEOMETRIES; $M_\infty = 3.97$, X = 8.50, L = 9.0, NO FINS.

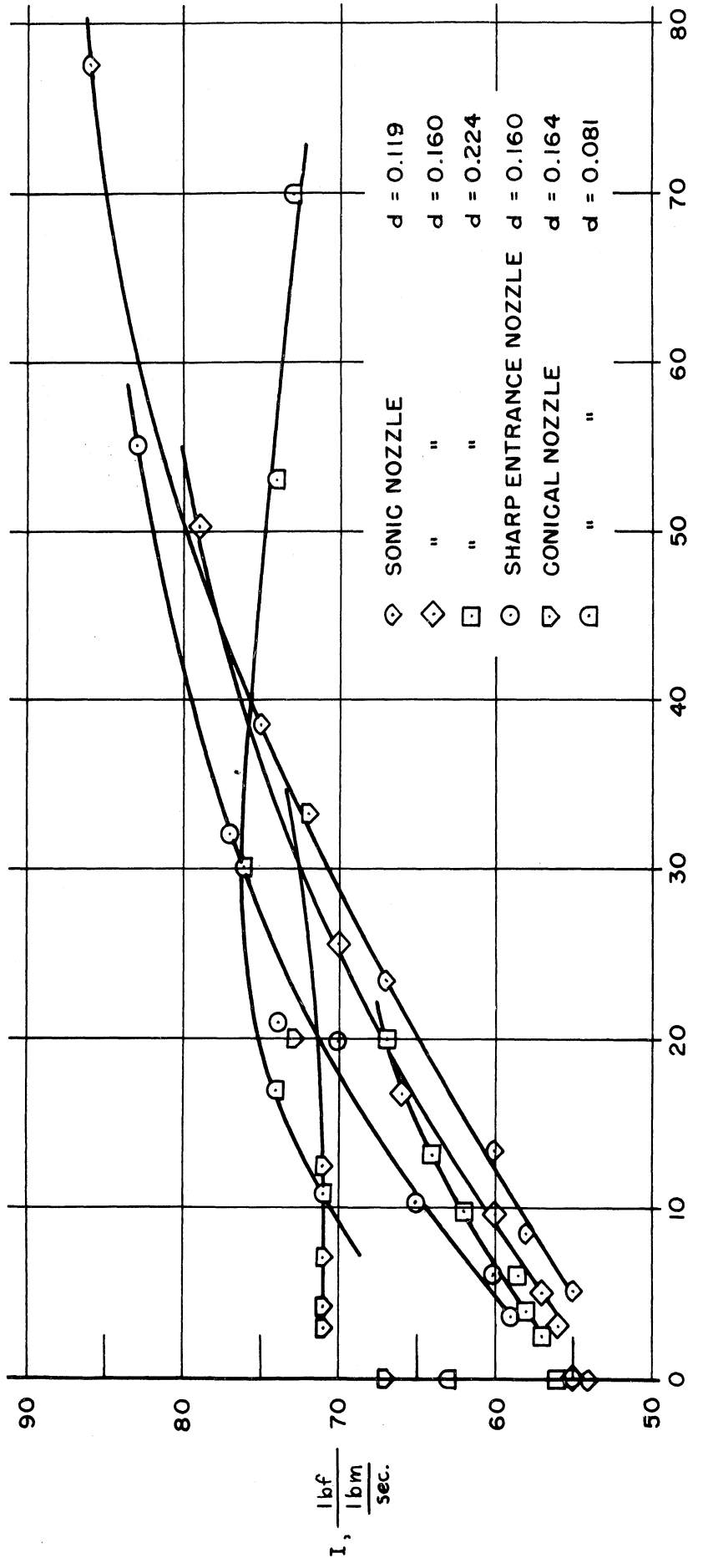

(b) IMPULSE VARIATION WITH MASS FLOW PARAMETER.

FIGURE 16. CONCLUDED.

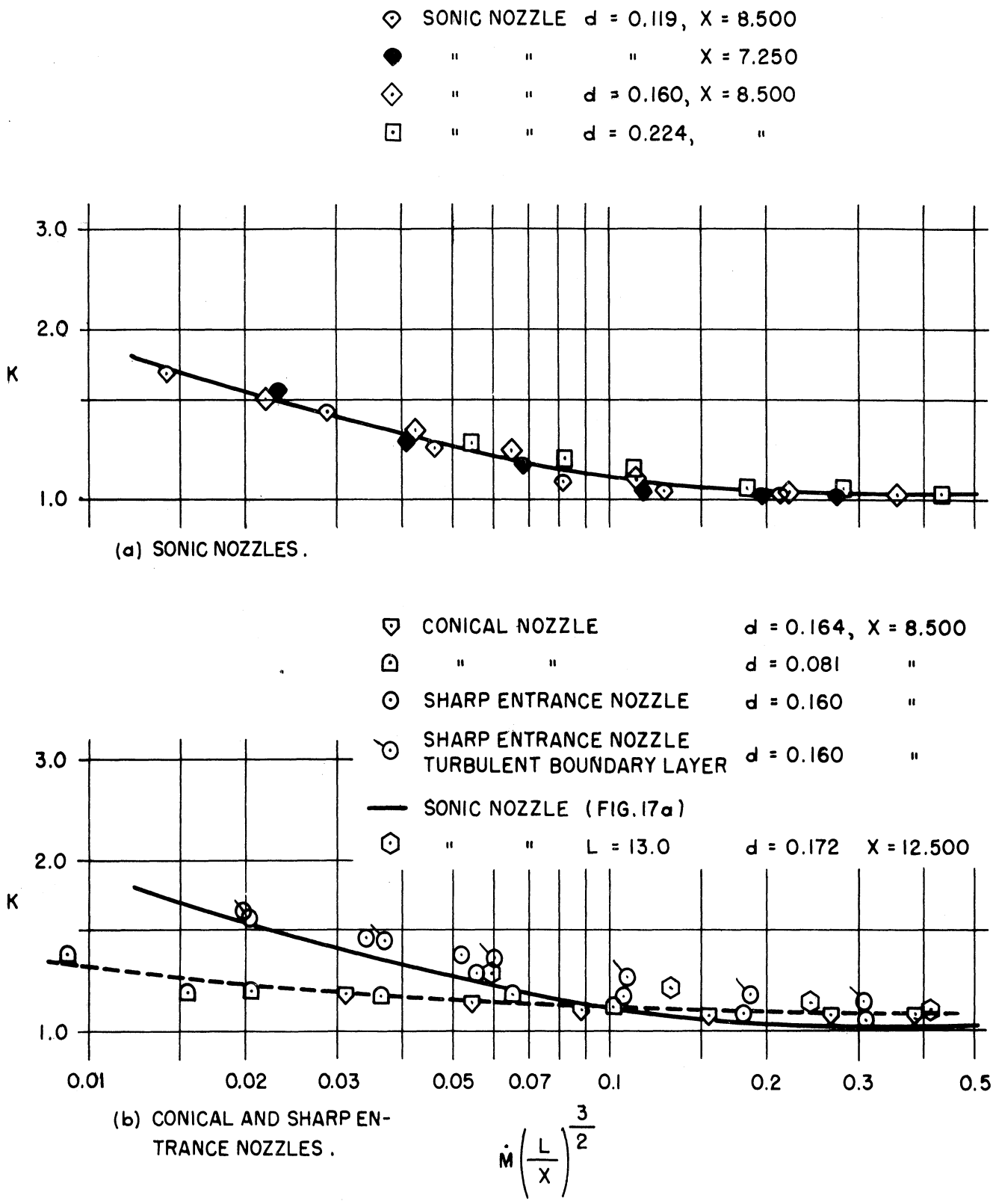

FIGURE 17. EFFECT OF NOZZLE GEOMETRY, AFTERBODY LENGTH AND BOUNDARY LAYER CONDITION ON MAGNIFICATION FACTOR; $M_\infty = 3.97$, L = 9.0, NO FINS.

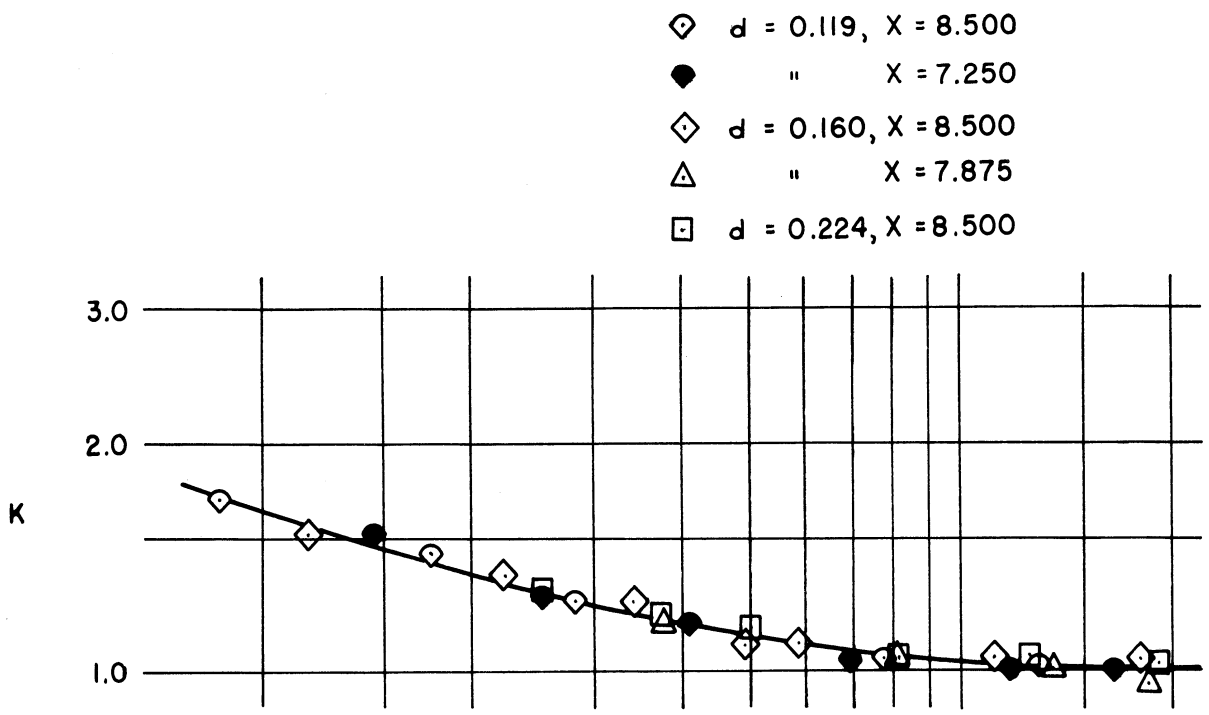

(a) PRESENT DATA; $M_\infty = 3.97$, L = 9.0, D = 2.00 .

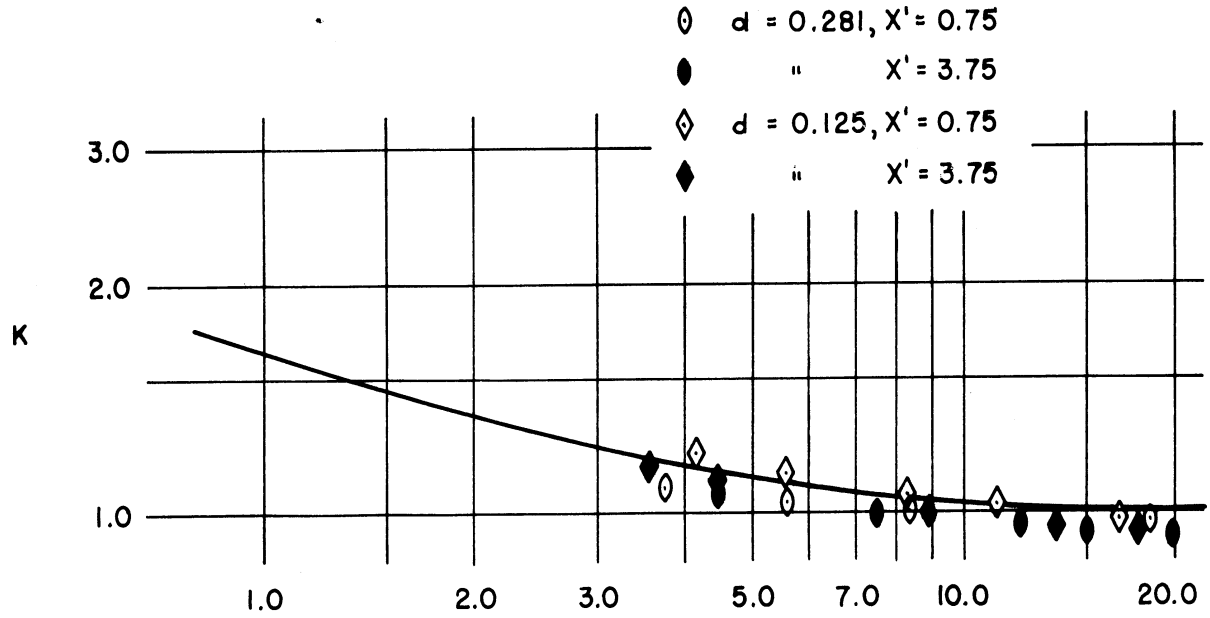

(b) COMPARISON OF PRESENT DATA (FIG. 18a) WITH DATA OF REFERENCE 3; $M_\infty = 3.99$, X = 7.4, D = 1.50. $\frac{P_{oj}}{P}\left(\frac{dL}{DX}\right)^{\frac{3}{2}}$

FIGURE 18. CORRELATION OF DATA FOR EFFECT OF NOZZLE GEOMETRY AND AFTERBODY LENGTH ON MAGNIFICATION FACTOR; NO FINS.

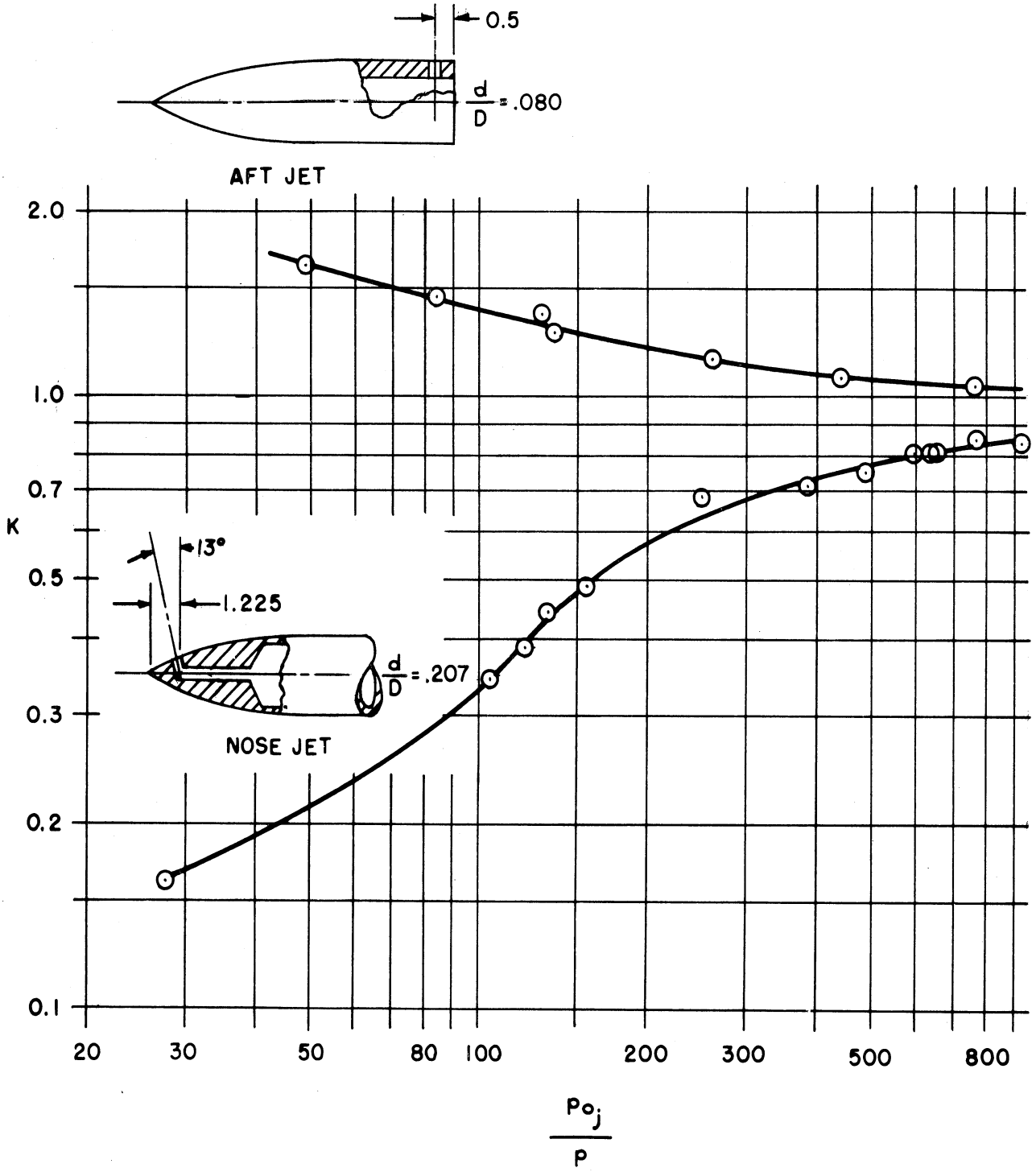

FIGURE 19. COMPARISON OF MAGNIFICATION FACTORS PRODUCED BY AFT AND NOSE-LOCATED SIDE-JETS; $M_\infty = 3.97$, d = 0.160, NO FINS.

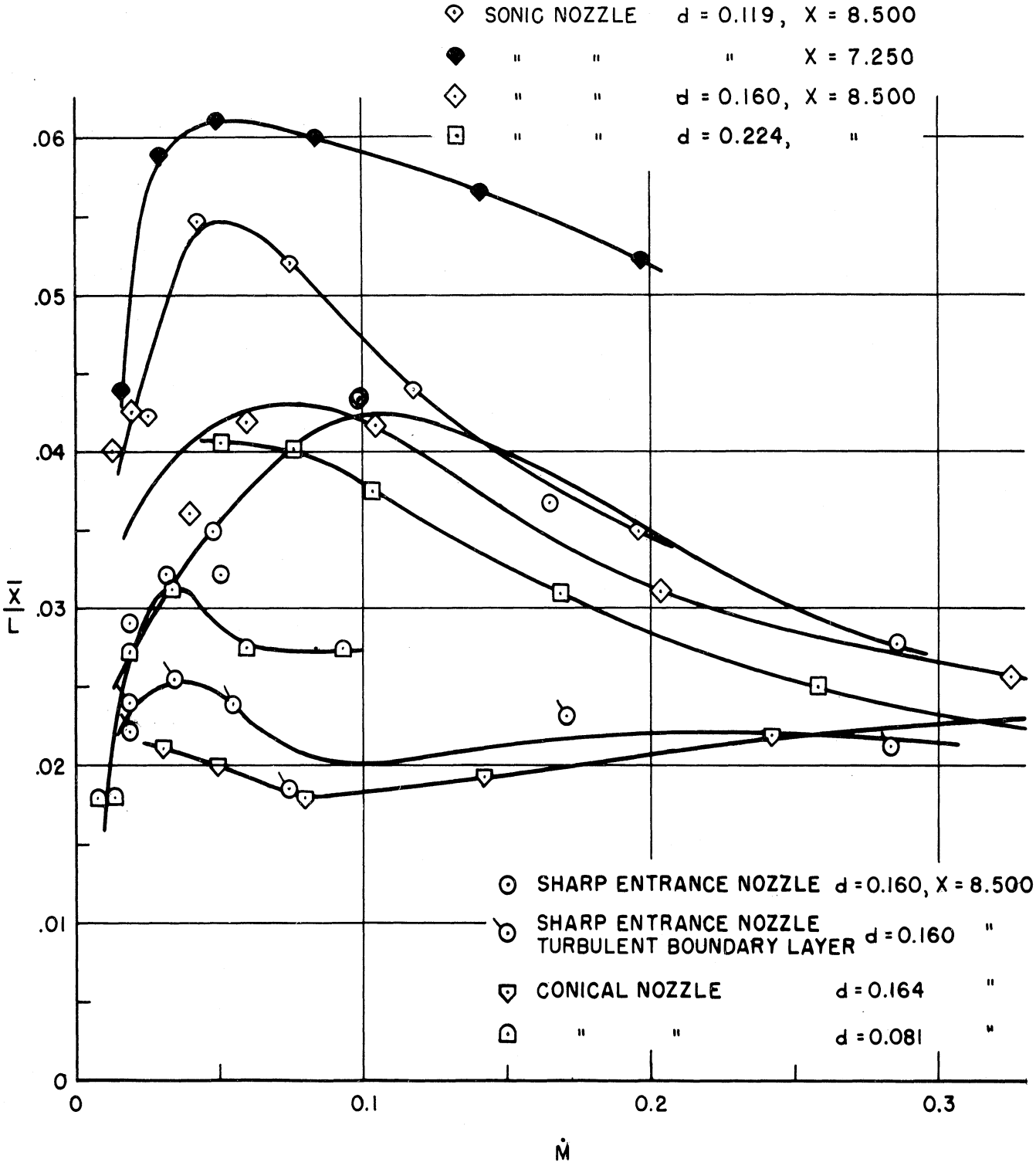

FIGURE 20. VARIATION OF CENTER OF PRESSURE OF TOTAL NORMAL FORCE WITH MASS FLOW PARAMETER FOR VARIOUS NOZZLE GEOMETRIES, AFTERBODY LENGTHS AND BOUNDARY LAYER CONDITIONS; $M_\infty = 3.97$, L = 9.0, NO FINS .

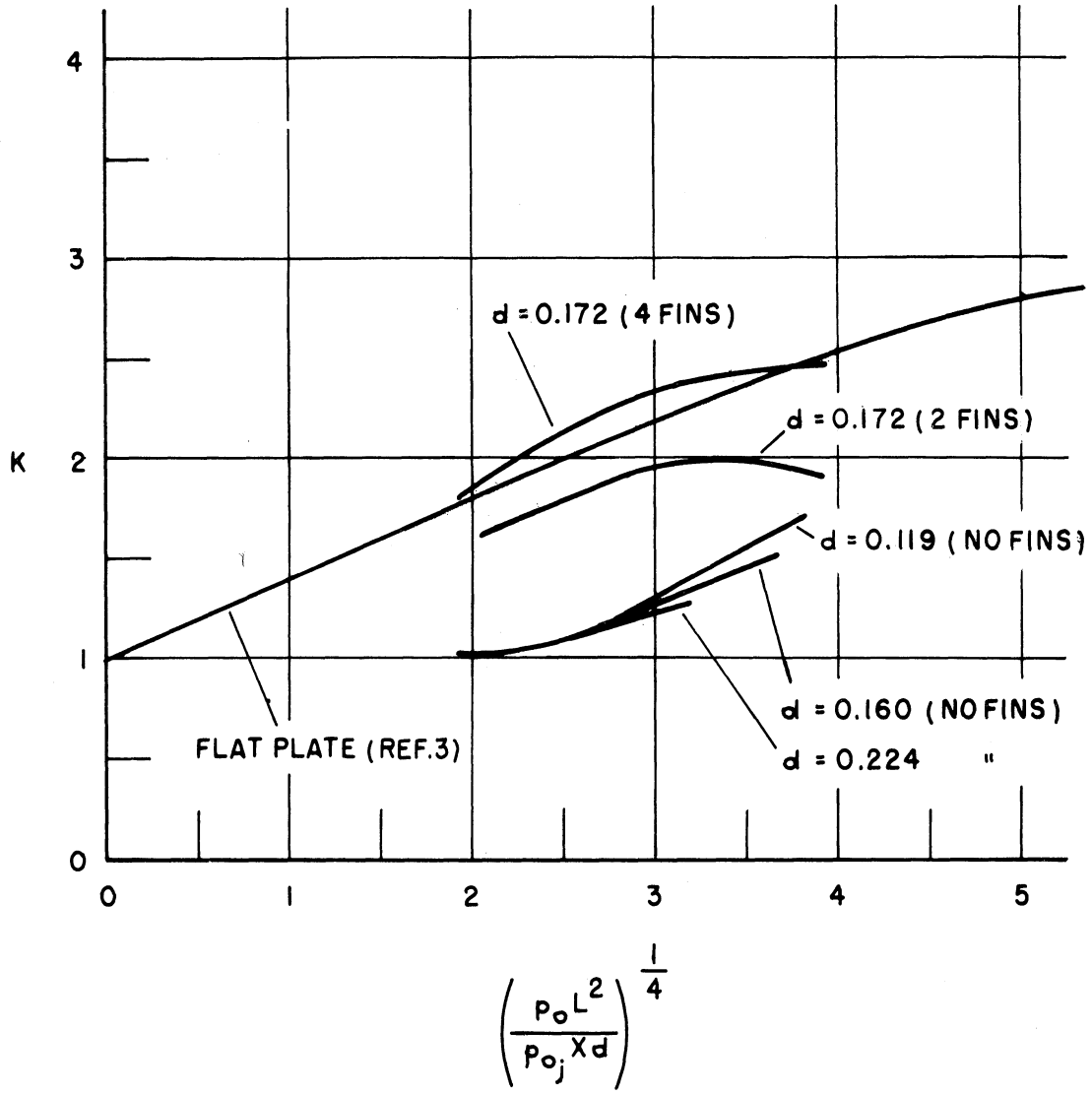

FIGURE 21. COMPARISON OF MAGNIFICATION FACTORS ON A FLAT PLATE AND BODY OF REVOLUTION; SONIC NOZZLES (FIN "C").

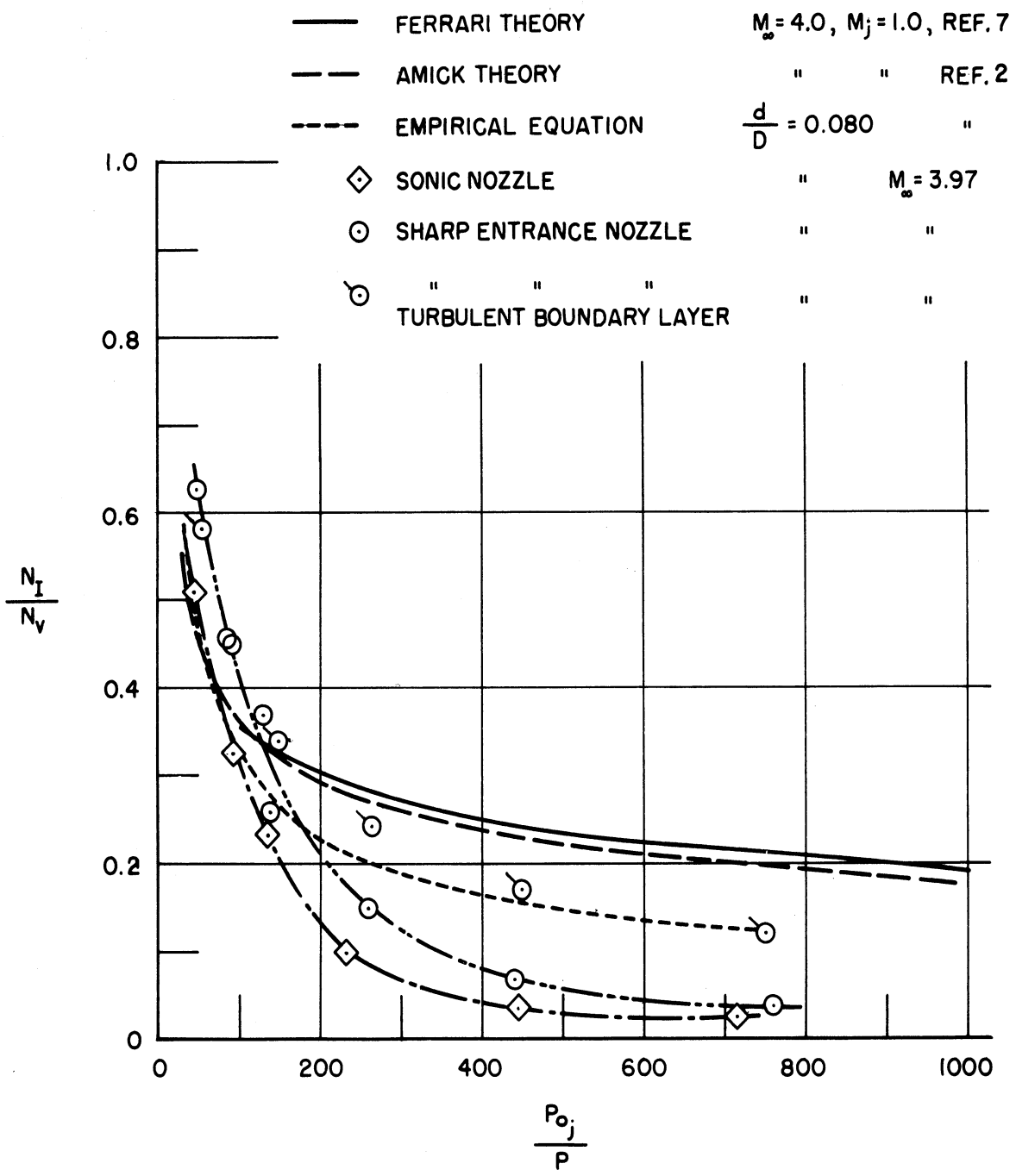

FIGURE 22. COMPARISON OF SIDE-JET INTERACTION THEORIES WITH EXPERIMENTAL RESULTS.

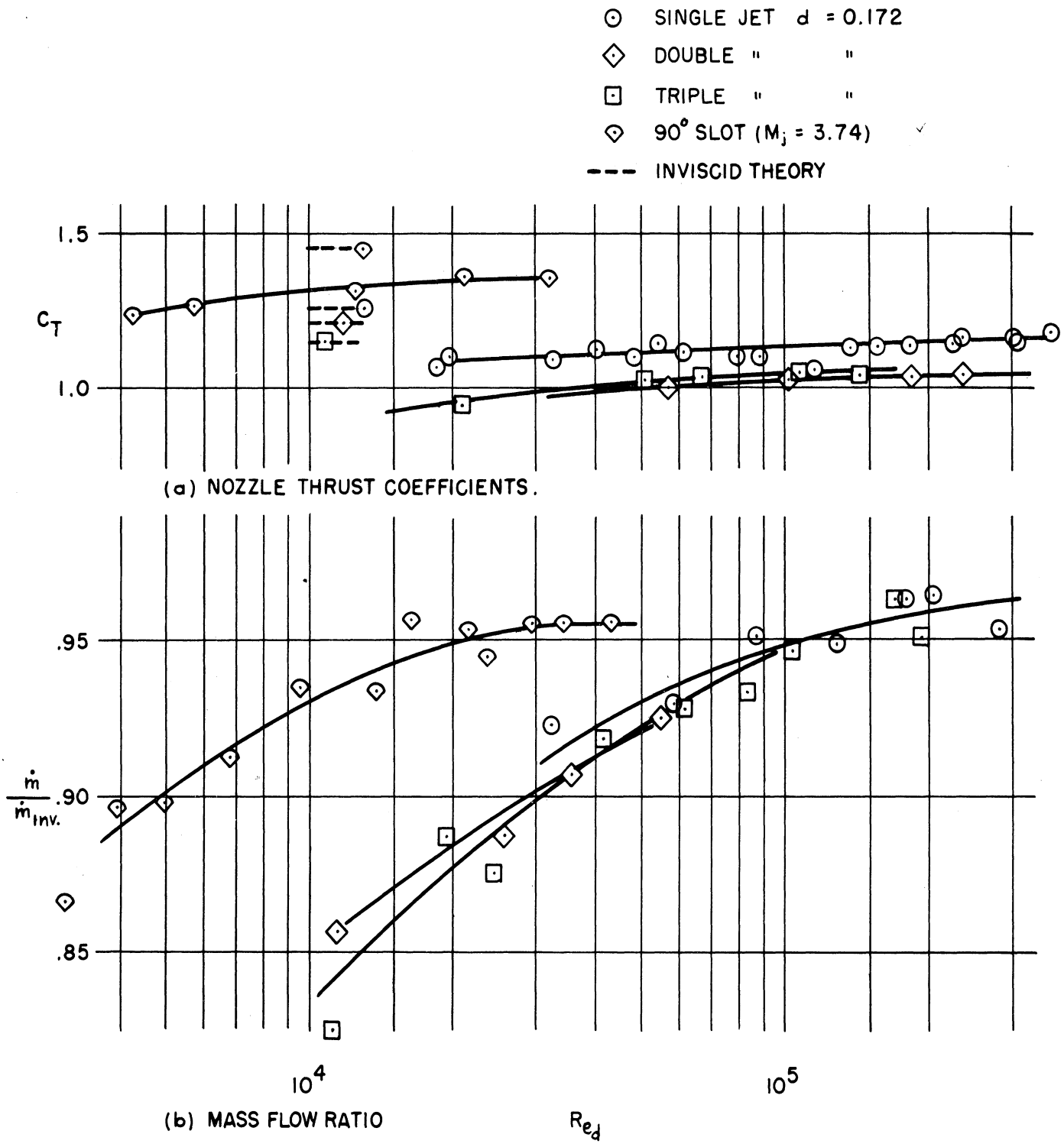

FIGURE 23. CALIBRATION CURVES FOR NOZZLES USED WITH BODY OF REVOLUTION - FIN CONFIGURATIONS.

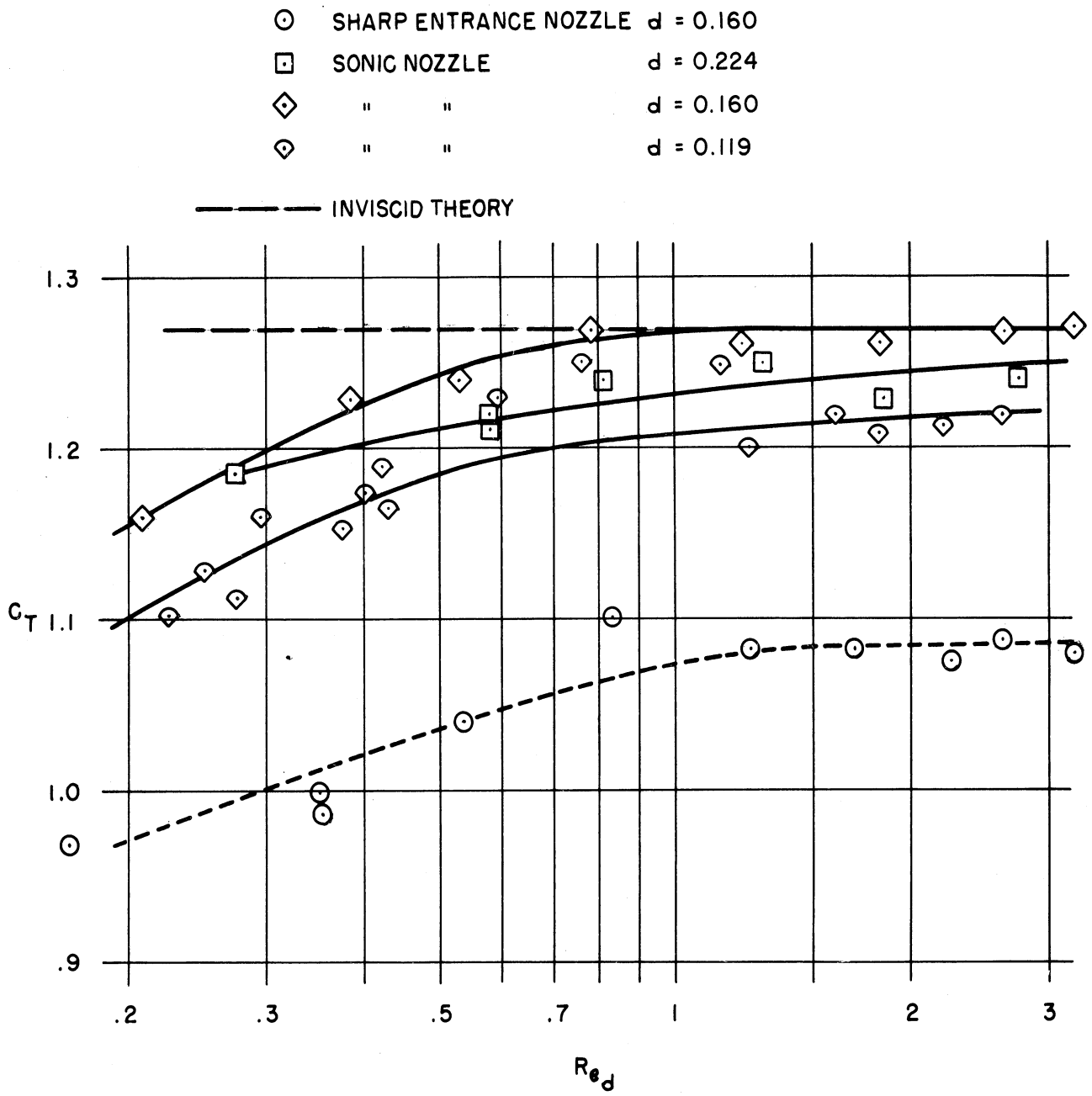

(a) THRUST COEFFICIENTS FOR SHARP ENTRANCE AND SONIC NOZZLES.

FIGURE 24. CALIBRATION CURVES FOR NOZZLES USED WITH BODY OF REVOLUTION WITHOUT FINS.

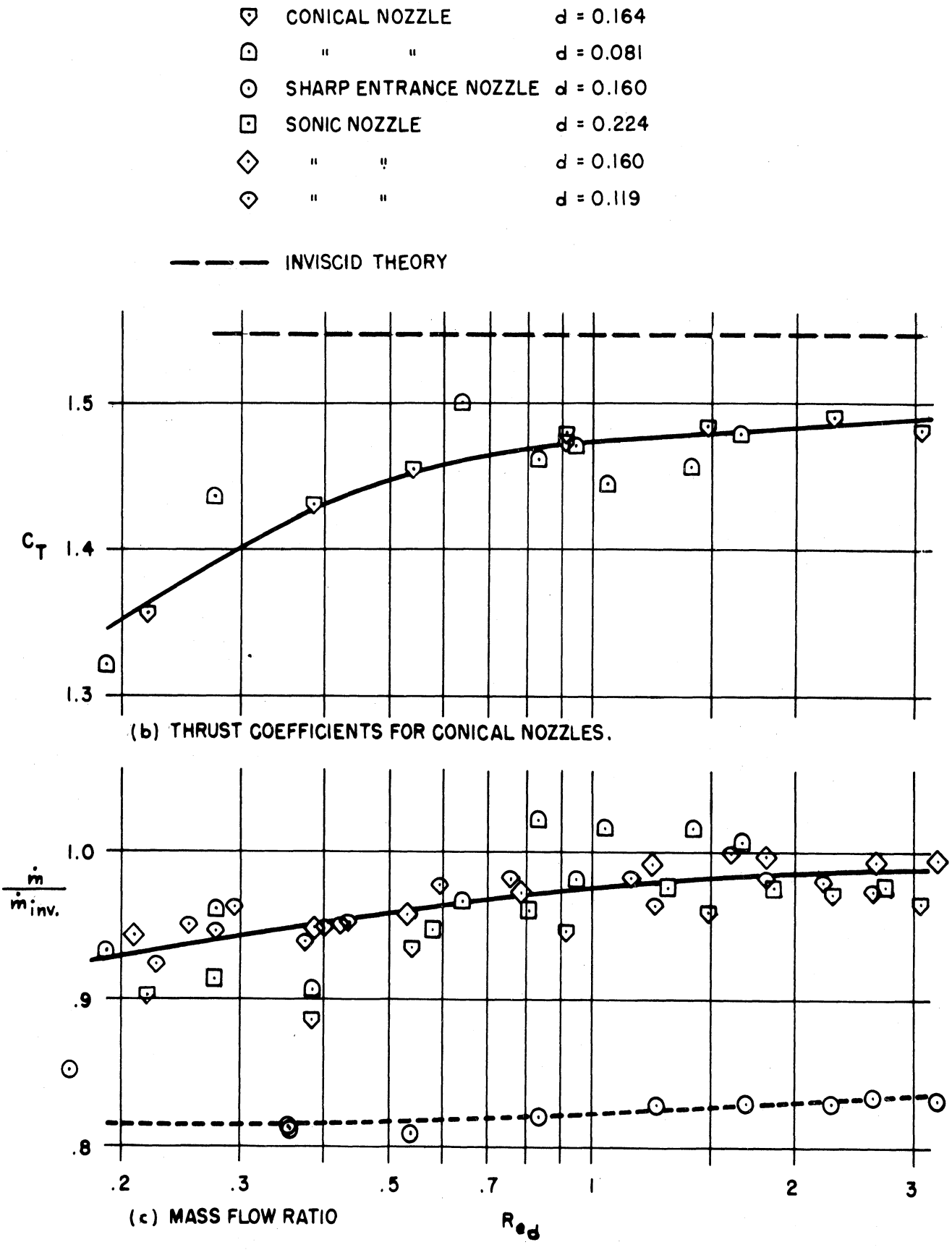

FIGURE 24. CONCLUDED.